Int J Earth Sci (Geol Rundsch) (2017) 106:283–309
DOI 10.1007/s00531-016-1319-y

ORIGINAL PAPER

Assessing the suitability of Holocene environments along the central Belize coast, Central America, for the reconstruction of hurricane records

Friederike Adomat[1] · **Eberhard Gischler**[1]

Received: 9 July 2015 / Accepted: 5 March 2016 / Published online: 26 March 2016

Abstract Since the Belize coast was repeatedly affected by hurricanes and the paleohurricane record for this region is poor, sediment cores from coastal lagoon environments along the central Belize coast have been examined in order to identify storm deposits. The paleohurricane record presented in this study spans the past 8000 years and exhibits three periods with increased evidences of hurricane strikes occurring at 6000–4900, 4200–3600 and 2200–1500 cal yr BP. Two earlier events around 7100 and 7900 cal yr BP and more recent events around 180 cal yr BP and during modern times have been detected. Sand layers, redeposited corals and lagoon shell concentrations have been used as proxies for storm deposition. Additionally, hiatuses and reversed ages may indicate storm influence. While sand layers and corals represent overwash deposits, the lagoon shell concentrations, which mainly comprise the bivalve *Anomalocardia cuneimeris* and cerithid gastropods, have been deposited due to changes in lagoon salinity during and after storm landfalls. Comparison with other studies reveals similarities with one record from Belize, but hardly any matches with other published records. The potential for paleotempestology reconstructions of the barrier–lagoon complexes along the central Belize coast differs depending on geomorphology, and deposition of washovers in the lagoon basins is limited, probably due to the interplay of biological, geological and geomorphological processes.

Keywords Paleotempestology · Tropical storms · Storm record · Overwash · Coastal lagoons · Shell concentrations

✉ Friederike Adomat
adomat@em.uni-frankfurt.de

[1] Institut für Geowissenschaften, J.W. Goethe Universität, 60438 Frankfurt am Main, Germany

Introduction and aims

The increase in intensity and destructiveness of hurricanes over the past few decades has been subject of discussions in a number of publications (e.g., Goldenberg et al. 2001; Emanuel 2005; Webster et al. 2005). The underlying causes for this phenomenon are not entirely clear; however, North Atlantic hurricane activity has been linked to increasing sea surface temperatures (SSTs) (Emanuel 2005; Hoyos et al. 2006; Saunders and Lea 2008; Donnelly et al. 2015), with an increase in frequency (Webster et al. 2005) and an increase in intensity of the strongest events (Elsner et al. 2008). The increase in SSTs since the late nineteenth century has been related to the sensitivity of Atlantic hurricanes to increasing atmospheric concentrations of greenhouse gasses (e.g., Emanuel 2005; Webster et al. 2005; Santer et al. 2006; Gillett et al. 2008; Knutson et al. 2010), internal climate variations (Goldenberg et al. 2001; Zhang and Delworth 2006, 2009) and reduced aerosol or dust forcing (Mann and Emanuel 2006; Evan et al. 2009). Simulations and modeling have yielded variability and uncertainties of hurricane activities, which may be associated with different model predictions (Emanuel et al. 2008). However, most studies agree that there will be century-scale increases in Atlantic tropical cyclone activity (e.g., Mann and Emanuel 2006; Holland and Webster 2007) and an increase in intensity and frequency of high-magnitude storms and a decrease in overall frequency of hurricanes by the end of the twenty-first century (Bender et al. 2010; Knutson et al. 2010).

As the most active area for tropical hurricanes in the North Atlantic (Donnelly 2005), the Caribbean is an area of interest for paleotempestology studies. The Belize coast, located in the western Caribbean, is vulnerable to hurricanes. The hurricane data (HURDAT), maintained

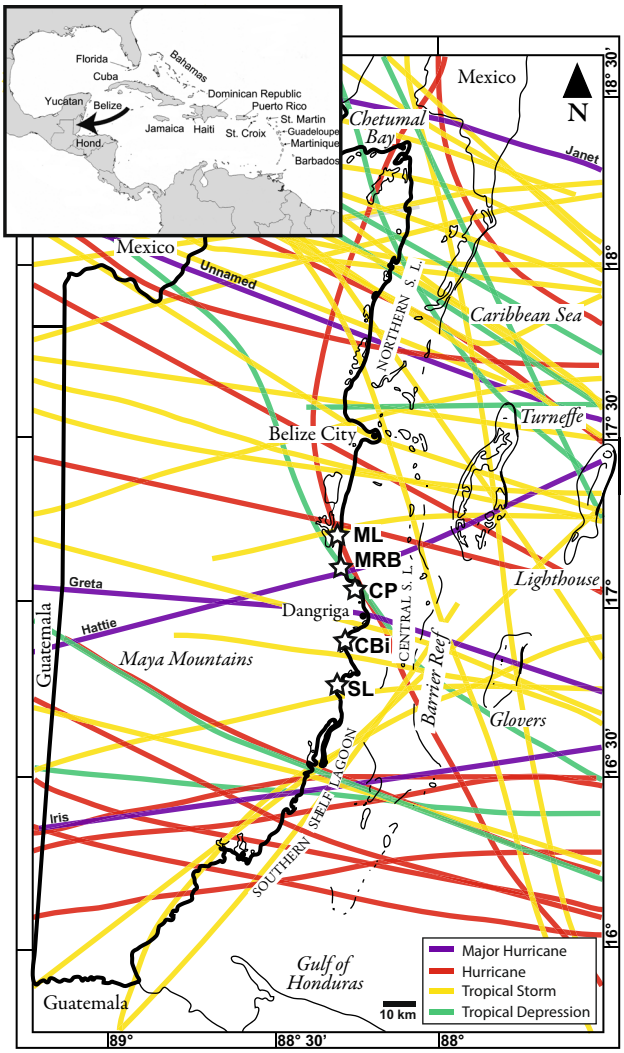

Fig. 1 Location map of Belize showing coring sites along the central coast of Belize. The *inset* map in the *upper left* shows the location of Belize in the Caribbean region (map after Montaggioni and Braithwaite 2009). *Asterisks* mark the localities Manatee Lagoon (*ML*), Colson Point Lagoon (*CP*), Commerce Bight Lagoon (*CBi*) and Sapodilla Lagoon (*SL*). Lines indicate approximate storm tracks recorded since 1851. Storm type refers to strength of storms during landfall at the coast. Storms are listed in Table 1. Source: U.S. National Hurricane Center (NOAA 2015)

by the National Oceanic and Atmospheric Administration (NOAA), provides Atlantic hurricanes and tropical storms recorded since 1851 (Fig. 1; Table 1). The terms major hurricane and intense hurricane refer to storms of category 3 or higher, according to the Saffir–Simpson scale. Storms affected northern and southern Belize more frequently than central Belize during recorded history. Density of storm tracks is highest in northern Belize and storm tracks typically run northwestward (Fig. 1). Since 1864, five major hurricanes of category 3 or higher and 14 hurricanes of categories 1 and 2 made landfall on the Belize coast. Major hurricanes include an unnamed hurricane in 1931, Janet in 1955, Hattie in 1961, Greta in 1978 and Iris in 2001. The major hurricane Keith, which struck Belize in 2000, weakened over the offshore Belize atolls and made landfall as a tropical storm. Major hurricanes Hattie and Greta impacted the study area in the vicinity of Mullins River Beach and Colson Point. Two hurricanes struck the Belize coast close to the study area, an unnamed in 1906 and Richard in October 2010.

Paleotempestology is an approach for assessing hurricane landfall probabilities by means of geological records of past hurricane strikes (Liu 2004). Storm records can be used to identify changes in hurricane climatology over the past years, also for the unrecorded time before 1851. Extending the historical and prehistoric record of tropical cyclone activity would support the ability to predict activity changes, including characteristics such as frequency, track, intensity and size that may occur in the future (Murnane 2004). Several geologic proxies have been used in paleotempestology. These include sediment-based proxies such as overwash deposits, wave- or flood-generated structures or deposits (tempestites) as well as micropaleontological proxies such as microfossils, and climatic proxies such as tree rings, oxygen isotherms from speleothems and corals (Liu 2004, and references therein). Paleohurricane records have mainly been generated by means of identification and analysis of overwash sand layers in sediment cores obtained from coastal wetlands, typically from coastal lakes, lagoons and marshes along the Atlantic U.S. coast (e.g., Donnelly et al. 2001a, b, 2004; Scott et al. 2003), the Gulf of Mexico (Liu and Fearn 1993, 2000a, b; Liu 2004; Lane et al. 2011; Brandon et al. 2013) and the Caribbean (Donnelly and Woodruff 2007; McCloskey and Keller 2009; Malaizé et al. 2011; McCloskey and Liu 2012). These records provide evidence of hurricane strikes dating back up to several thousand years and imply alternating periods of intense and reduced hurricane activity (e.g., Liu and Fearn 1993; Donnelly and Woodruff 2007; McCloskey and Liu 2012). However, storm records may be inconsistent among different regions (e.g., Mann et al. 2009). Stoddart (1962) and High (1969) documented geomorphological and sedimentological effects of hurricanes on Belize reefs and cays. Gischler et al. (2008, 2013) and Denommee et al. (2014) used coarse-grained layers intercalated in the muddy, annually laminated deposits of the offshore Blue Hole (Lighthouse Reef) to develop highly resolved storm records reaching back some 1.4 kyrs. But up to now only few studies have presented paleohurricane records obtained from the Belize coast (McCloskey and Keller 2009; McCloskey and Liu 2012). Aim of this study was to identify storm deposits in cores from the central Belize coast, to figure out active and quiet periods and to assess the results in comparison with other records in order to evaluate the

Table 1 Storms that struck the Belize coast recorded since 1851

Year	Date	Name	Area of Belize	Type (at landfall)	Wind (kt; max.)	Category
1864	Aug 26–Sep 1	–	Northern Belize	Hurricane	70	1
1870	Oct 30–Nov 30	–	Northern Belize	Hurricane	70	1
1892	Oct 5–16	–	Northern Belize	Hurricane	85	2
1893	Jul 4–7	–	Northern Belize	Hurricane	85	2
1898	Sep 12–22	–	Northern Belize	Tropical Storm	50	–
1898	Oct 27–Nov 4	–	Northern Belize	Tropical Storm	51	–
1904	Sep 28–Oct 4	–	Northern Belize	Tropical Storm	70	–
1906	Oct 8–23	–	Northern, Central B.	Hurricane	105	3
1916	Aug 27–Sep 2	–	Northern Belize	Tropical Storm	70	1
1917	Jul 6–14	–	Central Belize	Tropical Depression	45	–
1918	Aug 22–26	–	Southern Belize	Hurricane	90	2
1921	Jun 16–26	–	Northern Belize	Tropical Storm	80	1
1924	Jun 18–21	–	Northern Belize	Tropical Storm	40	–
1926	Oct 3–5	–	Southern Belize	Tropical Depression	35	–
1931	Jul 11–17	–	Northern Belize	Tropical Depression	60	–
1931	Aug 10–19	–	Central Belize	Tropical Storm	50	–
1931	Sep 6–13	–	Northern Belize	Major Hurricane	115	4
1931	Sep 8–16	–	Northern Belize	Tropical Storm	85	2
1931	Nov 11–16	–	Northern Belize	Tropical Storm	45	–
1932	Sep 25–Oct 2	–	Southern Belize	Tropical Storm	125	–
1932	Oct 7–15	–	Northern Belize	Tropical Storm	60	–
1933	Jul 14–24	–	Northern Belize	Tropical Storm	45	–
1933	Sep 16–25	–	Northern Belize	Tropical Storm	140	4
1934	Jun 4–18	–	Southern Belize	Tropical Storm	85	2
1938	Oct 10–17	–	Northern Belize	Tropical Storm	50	–
1940	Sep 18–25	–	Northern Belize	Tropical Storm	45	–
1941	Sep 23–30	–	Southern Belize	Hurricane	105	3
1942	Sep 15–22	–	Central Belize	Tropical Storm	45	–
1942	Nov 5–11	–	Northern Belize	Hurricane	85	2
1943	Oct 20–23	–	Southern Belize	Tropical Storm	40	–
1945	Aug 29–Sep 1	–	Northern Belize	Tropical Storm	50	–
1945	Oct 2–5	–	Southern Belize	Hurricane	85	2
1954	Sep 24–27	Gilda	Central Belize	Tropical Storm	60	–
1955	Sep 21–30	Janet	Northern Belize	Major Hurricane	150	5
1956	Sep 21–25	Flossy	Northern Belize	Tropical Depression	80	1
1960	Jul 10–16	Abby	Southern Belize	Hurricane	85	2
1961	Jul 20–24	Anna	Central Belize	Hurricane	100	3
1961	Oct 27–Nov 1	Hattie	Central Belize	Major Hurricane	140	5
1964	Nov 5–10	–	Northern Belize	Tropical Depression	35	–
1969	Aug 29–Sep 4	Francelia	Southern Belize	Hurricane	100	3
1971	Sep 5–18	Edith	Northern Belize	Tropical Storm	140	5
1971	Nov 12–22	Laura	Southern Belize	Tropical Storm	60	–
1974	Sep 14–22	Fifi	Southern Belize	Hurricane	95	2
1977	Oct 16–19	Frieda	Northern Belize	Tropical Depression	40	–
1978	Sep 13–20	Greta	Central Belize	Major Hurricane	115	4
1980	Sep 20–26	Hermine	Northern Belize	Tropical Storm	60	–
1993	Sep 14–21	Gert	Northern Belize	Tropical Storm	85	2
1999	Oct 28–Nov 1	Katrina	Northern Belize	Tropical Depression	35	–
2000	Sep 28–Oct 6	Keith	Northern Belize	Tropical Storm	120	4
2001	Aug 14–22	Chantal	Northern Belize	Tropical Storm	60	–

Table 1 continued

Year	Date	Name	Area of Belize	Type (at landfall)	Wind (kt; max.)	Category
2001	Oct 4–9	Iris	Southern Belize	Major Hurricane	125	4
2008	May 31–Jun 1	Arthur	Northern Belize	Tropical Storm	40	–
2010	Jun 25–Jul 2	Alex	Northern Belize	Tropical Storm	95	2
2010	Sep 23–26	Matthew	Southern Belize	Tropical Storm	50	–
2010	Oct 20–25	Richard	Central Belize	Hurricane	85	2
2011	Aug 19–22	Harvey	Central Belize	Tropical Storm	55	–
2013	Jun 17–20	Barry	Southern Belize	Tropical Depression	–	–

Tracks of storms are shown in Fig. 1

Source U.S. National Hurricane Center (NOAA 2015)

suitability of barrier–lagoon complexes for paleotempestology reconstructions.

Study area

Belize (16°S to 18°30′S; 87°30′W to 89°30′W) is situated in Central America, in the southeastern area of the Yucatán Peninsula, to the east bordered by the Caribbean Sea (Fig. 1). The climate is subtropical (Wright et al. 1959) and lies within the trade wind belt with prevailing easterly and northeasterly winds. The coast of Belize is a wave-dominated, semidiurnal microtidal area with a tidal range of 15–30 cm (Kjerfve et al. 1982). Annual rainfall increases from north to south from 124 to 380 cm, respectively (Purdy et al. 1975), reflecting mainland topography. Precipitation is highest during the summer (July–September). Drainage density is particularly high along the coast east of the Maya Mountains (High 1975); however, there are no systematical data available on river discharge. Mean sea surface temperatures of the shelf range from 28.9 °C during summer to 26.2 °C during winter (e.g., Purdy et al. 1975). Surface water salinity decreases from ca. 35 ‰ at the shelf margin to ca. 18 ‰ near the coast, and northward into Chetumal Bay and southward into the Gulf of Honduras (Purdy et al. 1975). Sedimentary facies of the shallow northern shelf are carbonate-dominated. The deeper southern shelf harbors a mixed system and is characterized by a siliciclastic to carbonate transition with an eastward increase in carbonate content (Pusey 1975; Scott 1975; Purdy et al. 1975; Purdy and Gischler 2003). The coast of Belize, which has low relief, is dominated by barrier–lagoon complexes (High 1966). The coastal lagoons are usually extensively fringed by the red mangrove *Rhizophora mangle*. The major processes supplying sediment to coastal environments include river transport, shore erosion, southerly longshore currents, tides, washovers and wind (Nichols and Boon 1994). Sediments delivered to the coast from the sea are mainly transported by longshore and tidal currents. Material from the hinterland is transported into coastal lagoons by creeks. The main sediment sources are the Maya Mountains and surrounding areas, where Paleozoic igneous, metamorphic and siliciclastic rocks and Cretaceous to Tertiary carbonates crop out. The coastal lowland is largely composed of unconsolidated Quaternary detrital sediments. A minor contributor is the offshore marine realm.

Today, muddy substrate and low current velocities predominate in the coastal lagoons selected for this study. Salinity in the lagoons, which hardly get deeper than about 1 m, is brackish and ranges from 4 to 27 ‰ (Adomat and Gischler 2015). (1) Manatee Lagoon is more than 10 km long and part of an even larger coastal lagoon system that is separated from the Belize shelf by an up to 2-km-wide swampy area with mangroves, bordered by a sand ridge with palm tree and palmetto vegetation and a seaward beach (Fig. 2a). The lagoon is connected with the sea by Manatee River. Quashi Trap Lagoon is a 2-km-long, shallow basin between Manatee Lagoon and the Belize shelf and connected to Manatee Lagoon by a shallow, ca. 500-m-long channel. (2) The Mullins River Beach area includes a swampy area bordered on the seaside by a sandy beach ridge (Fig. 2b). Much of the vegetation of the backshore area has recently been cleared for construction and connected with the Northern Highway to the west by an artificial causeway. (3) Colson Point Lagoon has a complex outline and is about 2 km wide (Fig. 2c). It is fed from the west by Big Creek and connected to the sea to the north by a complex system of strongly meandering and bifurcating creeks. A ca. 500-m-wide mangrove area separates the lagoon from the Belize shelf toward the east. (4) Commerce Bight has a more or less circular outline with an approximate diameter of 1.3 km and a pronounced tidal delta in the south (Fig. 2d). To the south, a ca. 2-km-long, small creek connects the lagoon basin with the adjacent Belize shelf. The width of the densely vegetated sandy ridge separating the lagoon from the sea is ca. 100 m. (5) Sapodilla Lagoon is an elongated, ca. 3-km-long lagoon with a ca. 135-m-wide inlet in the northeast that connects to the Belize shelf (Fig. 2e). It is separated from the shelf by a ca. 200-m-wide spit densely vegetated by mangroves.

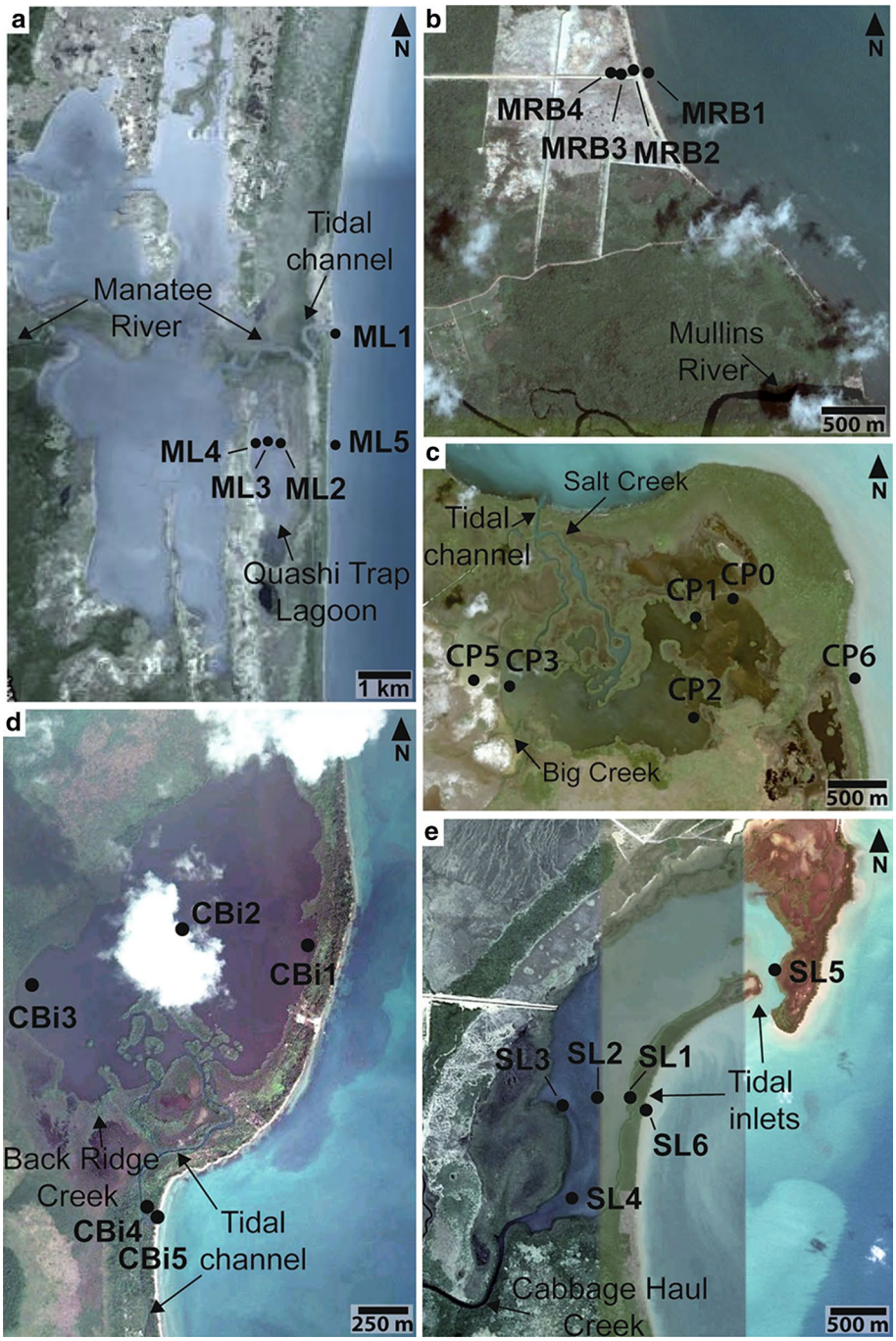

Fig. 2 Aerial photographs showing coring sites (satellite images from Google Earth). **a** Manatee Lagoon (Quashi Trap Lagoon). **b** Mullins River Beach. **c** Colson Point Lagoon. **d** Commerce Bight Lagoon. **e** Sapodilla Lagoon

The lagoon is fed by Cabbage Haul Creek entering at the southwestern lagoon margin.

Methods

Fieldwork took place in July and August 2011. A portable vibracorer (Lanesky et al. 1979) and 5.9-m-long aluminum tubes with a diameter of 7.5 cm, equipped with a copper core catcher, were used for coring. The five coring sites are located along the central Belize coast (Figs. 1, 2; Table 2). A total of 26 cores with a total length of 73 m were obtained. Core length ranged from 1.1 to 5 m. Compaction of sediment ranged between 0 and 65 %, with an average of 23 %. In the following, core depths are corrected for compaction by multiplying thicknesses of all sediment types with the compaction factor obtained from core depth and penetration depth (Table 2). One compaction factor was calculated for each core. In the laboratory, core tubes were cut in halves lengthwise using an angle

Table 2 List of all cores drilled at Manatee Lagoon (ML), Mullins River Beach (MRB), Colson Point Lagoon (CP), Commerce Bight Lagoon (CBi) and Sapodilla Lagoon (SL)

Core	Coordinates		Water depth (cm)	Core length (cm)	Penetration depth (cm)	Compaction (%)
	Latitude	Longitude				
ML 1	N 17°13′50.3″	W 88° 18′13.5″	40	122.5	349	64.90
ML 2	N 17° 12′41.5″	W 88° 18′46.2″	57	452	478	5.44
ML 3	N 17° 12′41.8″	W 88° 18′53.3″	93	274	302	9.27
ML 4	N 17° 12′41.0″	W 88° 19′03.2″	73	437	464	5.82
ML 5	N 17° 12′39.8″	W 88° 18′13.8″	100	432	500	13.60
MRB1	N 17° 07′11.4″	W 88° 18′00″	81	394	499	21.04
MRB2	N 17° 07′11.6″	W 88° 18′02.2″	+100[a]	344	456	24.56
MRB3	N 17° 07′10.5″	W 88° 18′05.5″	0	269	305	11.80
MRB4	N 17° 07′10.6″	W 88° 18′06.6″	0	297	366	18.85
CP 0	N 17° 03′37.6″	W 88° 15′11.8″	58	318	338	5.90
CP 1	N 17° 03′25.7″	W 88° 15′22.2″	64	261	343	23.90
CP 2	N 17° 03′04.3″	W 88° 15′48.1″	88	168	257	34.60
CP 3	N 17° 03′12.9″	W 88° 16′13.6″	72	264	360	26.70
CP 5	N 17° 03′27.1″	W 88° 16′26.8″	57	99	109	9.17
CP 6	N 17° 03′15.3″	W 88° 14′37.9″	50	206	307	32.90
CBi 1	N 16° 54′04.5″	W 88° 16′55.9″	78	244	285	14.40
CBi 2	N 16° 54′08.2″	W 88° 17′17.0″	102	228	251	9.20
CBi 3	N 16° 53′55.3″	W 88° 17′42.2″	76	179	179	0.00
CBi 4	N 16° 53′18.6″	W 88° 17′22.7″	56	154	286	46.20
CBi 5	N 16° 53′18.1″	W 88° 17′21.6″	12	220	458	51.90
SL 1	N 16° 45′52.4″	W 88° 18′47.7″	109	271	366	26.00
SL 2	N 16° 45′52.5″	W 88° 18′58.3″	96	238	384	38.00
SL 3	N 16° 45′50.8″	W 88° 19′08.0″	78	325	453	28.26
SL 4	N 16° 45′22.0″	W 88° 19′05.8″	69	256	386	33.68
SL 5	N 16° 46′30.4″	W 88° 18′01.9″	94	457	489	26.18
SL 6	N 16° 45′48.4″	W 88° 18′43.7″	109	388	440	11.80

[a] Elevation estimated

grinder and knife. Photograph documentation and core description were carried out, including descriptions of lithology, thickness, sedimentary structures and sedimentary contacts. Potential event deposits were identified by visual examination of cores and based on sediment texture (sieve analysis). Sediment was washed through 2- and 1-mm, and 500-, 250-, 125- and 63-µm sieves for grain size analysis and to isolate shells from the sediment. Samples of organic matter, bivalve shells and corals were selected to date possible event deposits. Age-dating was undertaken by Beta Analytic Inc., Miami, Florida, using accelerator mass spectrometry (AMS). Radiocarbon ages were converted to calendar years using Intcal09 (Talma and Vogel 1993). Calibrated ages are given with a 2 σ error range. For calibration of carbonate shells, the Marine09 database was applied, and for peat and organic sediments, the Intcal09 database was applied. The variables used in the calculation for marine reservoir effect correction of carbonate shells are Delta-R = 120 ± 27 and Glob res = −200 to 500. A complete list of the radiocarbon ages is shown in Table 3.

Results

Sediments

Holocene and Pleistocene sediments were recovered in the vibracores (Adomat and Gischler 2015). Facies successions and distribution do not show uniform patterns but strong local variation. Sediments comprise Holocene peat and peaty sediment, mud, sand and poorly sorted sediments. Pleistocene soils form the basement of Holocene sediments. Coastal lagoon evolution started around 6 kyrs BP. Lagoon cores are predominantly composed of mud and peat units with mangrove roots and occasional shell concentrations. From north to south, the major characteristics

Table 3 List of accelerator mass spectrometry ^{14}C ages reported by Beta Analytic Inc., Miami, Florida (Adomat and Gischler 2015)

Core	Sample (uncorrected depth below core top, in cm)	Dated material	Depth below sea level (corrected for compaction, in cm)	Measured age (year BP) ± 1σ	$^{13}C/^{12}C$ ratio (‰)	Conventional age (yr BP)	Calibrated calendar age, (cal yr BP, 2 σ range)	BETA no.
ML1	55–58	Organic matter	201	690 ± 30	−24.3	700 ± 30	665 ± 15, 575 ± 5	325007
ML1	102–107	Bivalve shell	338	1750 ± 30	−4.6	2080 ± 30	1500 ± 100	348282
ML2	0–5	Bivalve shell	60	124.2 ± 0.4 (pMC)	−0.4	118.2 ± 0.4	Modern	348283
ML2	74–75	Organic matter	139	3900 ± 30	−25.5	3890 ± 30	4330 ± 90	325008
ML2	103–105	Bivalve shell	167	5030 ± 30	−4.3	5370 ± 30	5620 ± 60	348284
ML2	159–162	Bivalve shell	233	1740 ± 30	−6.4	2050 ± 30	1470 ± 90	325009
ML3	17–22	Bivalve shell	114	3540 ± 30	−7.7	3820 ± 30	3610 ± 90	348285
ML3	27–28	Organic matter	123	3820 ± 30	−26.3	3800 ± 30	4275 ± 5, 4195 ± 55, 4110 ± 20	325010
ML3	99–104	Bivalve shell	205	4730 ± 30	−4	5070 ± 30	5315 ± 85	325011
ML4	20–25	Bivalve shell	118	109.9 ± 0.3 (pMC)	−2.5	105 ± 0.3	Modern	348286
ML5	60–65	Bivalve shell	173	290 ± 30	−1.1	680 ± 30	180 ± 100	325012
ML5	425–426	Organic matter	494	5920 ± 40	−26.4	5900 ± 40	6725 ± 75, 6645 ± 5	325013
MRB1	38–43	Bivalve shell	132	107.5 ± 0.3 (pMC)	+0.4	102 ± 0.3	Modern	348287
MRB1	222–223	Organic matter	363	7100 ± 40	−28.2	7050 ± 40	7875 ± 85	345343
MRB1	229–230	Organic matter	372	7190 ± 40	−27	7160 ± 40	7980 ± 40	345344
MRB2	255–256	Organic matter	239	6250 ± 30	−30.3	6160 ± 30	7055 ± 105	345345
MRB2	296–297	Organic matter	293	6940 ± 40	−24.4	6950 ± 40	7910 ± 10, 7770 ± 90	345346
MRB3	179	Organic matter	203	6310 ± 40	−25.8	6300 ± 40	7235 ± 75	345347
MRB3	267–269	Organic matter	304	3160 ± 30	−26.0	3140 ± 30	3435 ± 5, 3370 ± 30, 3280	345348
MRB4	243–244	Organic matter	300	6070 ± 40	−26.4	6050 ± 40	6895 ± 105	345349
CP0	33–38	Bivalve shell	96	1730 ± 30	−2.9	2090 ± 30	1510 ± 100	238280
CP0	105–110	Bivalve shell	172	3940 ± 30	−5	4270 ± 30	4215 ± 125	348281
CP1	70–75	Bivalve shell	159	2280 ± 30	−2.6	2650 ± 30	2200 ± 100	307038
CP1	86–88	Organic matter	178	3610 ± 30	−24.4	3620 ± 30	4055 ± 5, 3920 ± 70	307039
CP1	187–192	Bivalve shell	312	5400 ± 30	−6.7	5700 ± 30	5985 ± 105	307040
CP2	5–10	Bivalve shell	99	2200 ± 30	−3.1	2560 ± 30	2070 ± 90	307041
CP2	20–25	Bivalve shell	122	2200 ± 30	−1.6	2580 ± 30	2115 ± 125	307042
CP2	40–45	Organic matter	153	3420 ± 30	−26.2	3400 ± 30	3634 ± 65	307043
CP3	5–10	Bivalve shell	82	150 ± 30	−2.7	520 ± 30	Modern	307044
CP6	52–57	Bivalve shell	131	30 ± 30	−1.1	420 ± 30	Modern	307045
CP6	89	Coral	183	560 ± 30	−4.7	890 ± 30	390 ± 90	307046
CP6	119–121	Organic matter	229	4530 ± 30	−23.8	4550 ± 30	5295 ± 25, 5220, 5150 ± 30, 5085 ± 25	307047

Table 3 continued

Core	Sample (uncorrected depth below core top, in cm)	Dated material	Depth below sea level (corrected for compaction, in cm)	Measured age (year BP) ± 1σ	$^{13}C/^{12}C$ ratio (‰)	Conventional age (yr BP)	Calibrated calendar age, (cal yr BP, 2 σ range)	BETA no.
CP6	130–135	Bivalve shell	247	4370 ± 30	−4	4710 ± 30	4815 ± 45	307048
CBi1	157–160	Coral	263	4500 ± 30	−3.6	4850 ± 30	4945 ± 105	317594
CBi1	169–170	Organic matter	276	4380 ± 30	−27	4350 ± 30	5025 ± 5, 4910 ± 60	317595
CBi1	212–213	Organic matter	327	4720 ± 30	−28.7	4660 ± 30	5390 ± 80	317596
CBi1	243–244	Peat	363	4860 ± 40	−25.6	4850 ± 40	5615 ± 35, 5525 ± 5, 5500 ± 20	317597
CBi2	47–48	Organic matter	154	4080 ± 30	−25.2	4080 ± 30	4780 ± 20, 4685 ± 5, 4580 ± 60, 4460 ± 10	348278
CBi2	84–85	Organic matter	195	3560 ± 30	−26.3	3540 ± 30	3855 ± 45, 3760 ± 40	317598
CBi4	38	Bivalve shell	127	115.5 ± 0.3	−3.7	110.6 ± 0.3	Modern	348279
CBi4	100–101	Organic matter	243	80 ± 30	−28	30 ± 30	Modern	317599
CBi4	107–112	Coral	260	1820 ± 30	−6	2130 ± 30	1585 ± 95	317600
CBi4	153–154	Organic matter	342	1630 ± 30	−22.6	1670 ± 30	1680 ± 10, 1570 ± 50	317601
CBi5	125–130	Coral	277	1140 ± 30	−3	1500 ± 30	925 ± 65	317602
CBi5	153–158	Coral	335	2810 ± 30	−5.5	3130 ± 30	2780 ± 70	317603
CBi5	208–213	Coral	450	1860 ± 30	−3.2	2220 ± 30	1675 ± 105	317604
SL1	40–45	Bivalve shell	166	320 ± 30	−3.9	670 ± 30	Modern	348288
SL1	220–225	Bivalve shell	409	3710 ± 30	−0.1	4120 ± 30	4005 ± 115	320754
SL1	240–241	Peat	434	5790 ± 40	−27	5760 ± 40	6555 ± 105	320755
SL2	214–216	Peat	442	5290 ± 30	−26.2	5270 ± 30	6160 ± 20, 6050 ± 70, 5960 ± 20	320756
SL3	211–212	Organic matter	372	5420 ± 30	−28.1	5370 ± 30	6255 ± 25, 6200 ± 20, 6130 ± 20, 6070 ± 10, 6035 ± 15	320757
SL4	150–155	Bivalve shell	299	1260 ± 30	−0.8	1660 ± 30	1080 ± 90	320758
SL4	199–200	Peat	370	5180 ± 40	−26.4	5160 ± 40	5975 ± 15, 5920 ± 30, 5795 ± 5, 5775 ± 5	320759
SL5	46–51	Bivalve shell	146	830 ± 30	+0.5	1250 ± 30	680 ± 50	320760
SL5	270–275	Bivalve shell	386	5340 ± 30	+0.9	5760 ± 30	6040 ± 120	348292
SL5	452–457	Bivalve shell	580	3580 ± 30	+1.9	4020 ± 30	3880 ± 90	320761
SL6	91–96	Bivalve shell	215	1730 ± 30	+0.6	2150 ± 30	1600 ± 90	320762
SL6	360–361	Organic matter	516	4750 ± 30	−26.6	4720 ± 30	5545 ± 35, 5465 ± 25, 5365 ± 45	320763

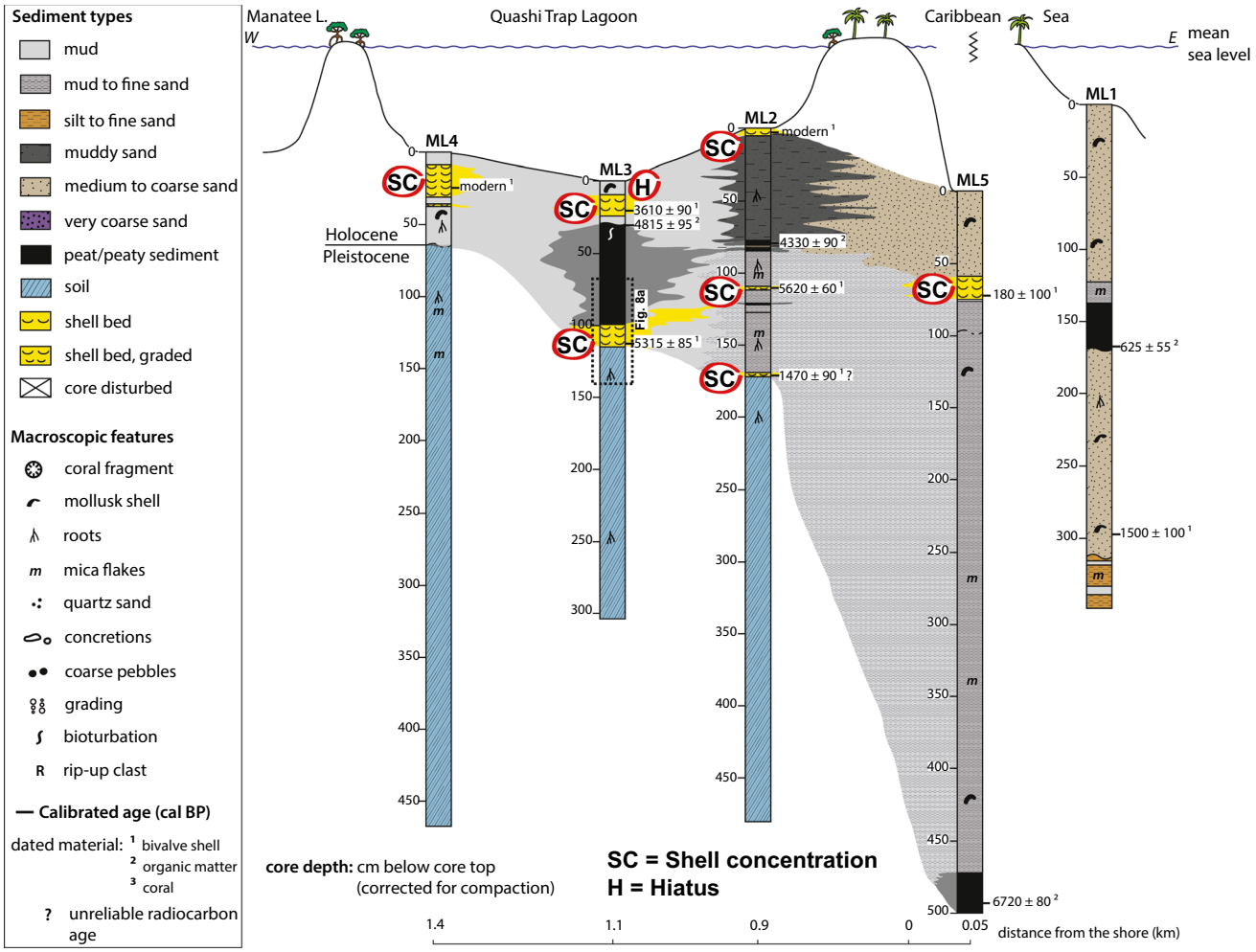

Fig. 3 Core logs and interpreted sedimentary facies at Manatee Lagoon. Location of coring sites is shown in Fig. 2. Core logs were corrected for compaction and are arranged with reference to the sea level. Abbreviations highlight deposits, which are interpreted to be related to hurricanes. *SC* shell concentration. *Dashed rectangle* in ML3 highlights core section shown in Fig. 8

of the sedimentary successions are as follows: In Manatee Lagoon, the Pleistocene basement dips toward the sea and is overlain by mud with shell concentrations (Fig. 3). Silt to fine sand and muddy sand occurs in the most seaward lagoon core. Cores from the marginal area show barrier sand, which overlie mud to fine sand. At Mullins River Beach, mud predominates, which may have been deposited in a reed swamp (Fig. 4). In some core sections, sand and laminated sediment were observed. Holocene sediments from Colson Point Lagoon predominantly comprise mud with shell concentrations, which is intercalated by mangrove peats and peaty sediments (Fig. 5). The underlying Pleistocene deposits exhibit considerable relief. In Commerce Bight Lagoon, mud overlies muddy sands (Fig. 6). In the backbarrier core, sand alternates with silt to fine sand. The channel deposits comprise largely medium to coarse sand, which overlie micaceous silt to fine sand. Sediments from Sapodilla Lagoon consist of thick lagoonal muds and Holocene basal peats and peaty sediments (Fig. 7). Close to the river mouth (SL4) and the tidal inlets (SL5, SL6), coarse-grained sediments occur.

Possible storm deposits and radiocarbon dating

Possible storm deposits have been identified in 18 cores from the five localities. These include sand layers marine fauna, shell concentrations, hiatuses and reversed ages (Tables 4, 5). Radiocarbon dating of the sand layers has proven difficult because no appropriate material for radiocarbon dating was found. To obtain an approximate age of the sand deposits, organic matter from the top of the underlying sediments was selected for dating. This way, four of five sand layers have been dated. Further radiocarbon ages have been obtained from five corals and from bivalves from 15 of 17 shell concentrations. The basal concentration in CP6 and the concentration in CBi3 were not age-dated.

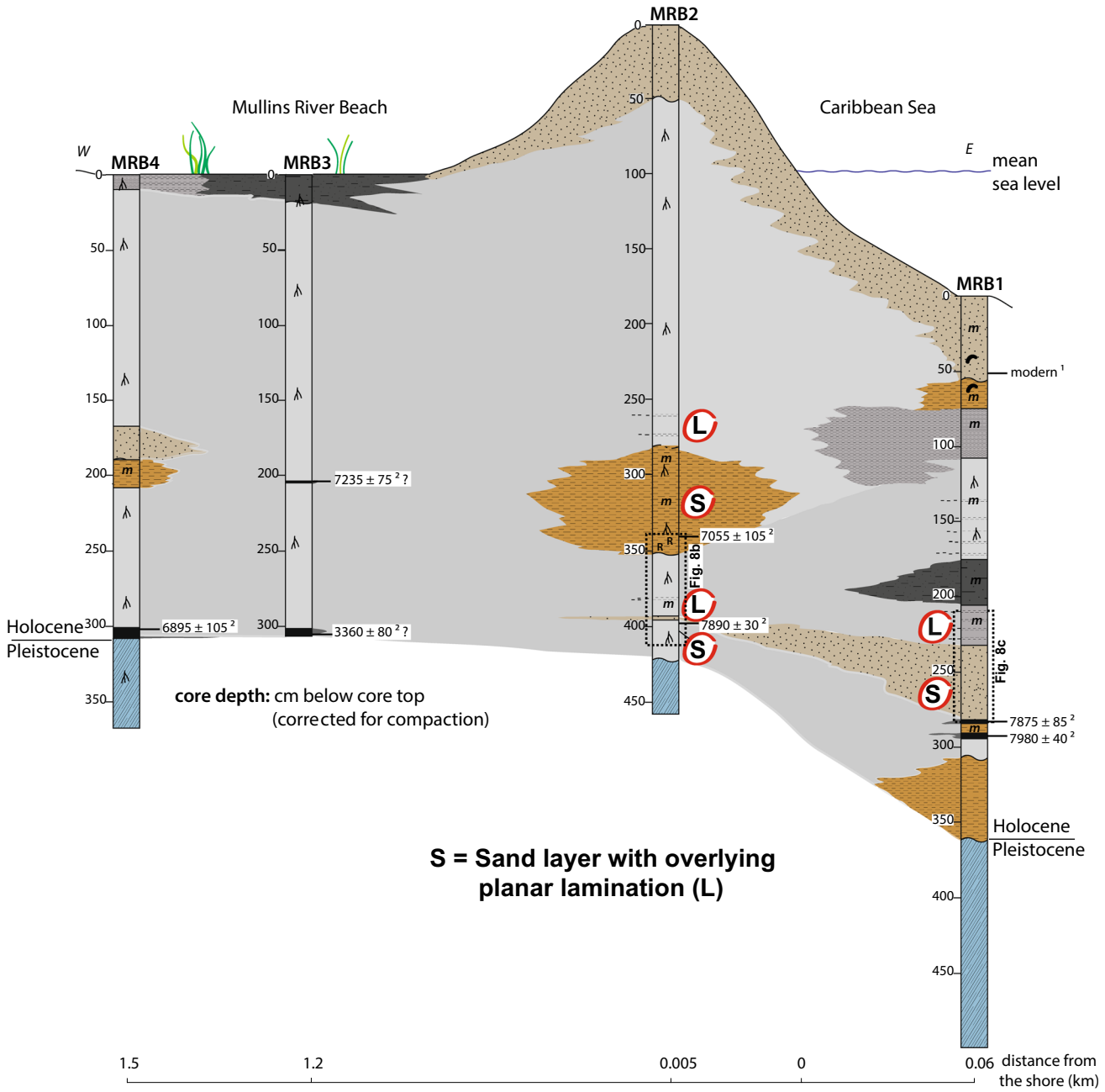

Fig. 4 Core logs and interpreted sedimentary facies at Mullins River Beach. Location of coring sites is shown in Fig. 2. Core logs were corrected for compaction and are arranged with reference to the sea level. Abbreviations highlight deposits, which are interpreted to be related to hurricanes. *L* planar lamination, *S* sand. *Dashed rectangles* in MRB1 and MRB2 highlight core sections shown in Fig. 8

Articulated bivalve shells and corals preserved in situ potentially to be used for dating were not available.

Manatee Lagoon

In cores from Manatee Lagoon, seven shell concentrations were observed in the lagoonal cores ML2, ML3 and ML4 (Figs. 3, 8a). Mollusk fauna within the lagoonal shell concentrations mainly comprise the bivalve *Anomalocardia cuneimeris* and cerithid gastropods (Adomat et al. 2016). Besides Manatee Lagoon, lagoonal shell concentrations were also found in cores from Colson Point, Commerce Bight and Sapodilla Lagoon. Based on statistical analyses, seven assemblages were distinguished for these lagoonal concentrations. Assemblage A1 comprises mainly *A. cuneimeris* and *C. eburneum*. In A2 and A3, the dominant species is *A. cuneimeris*. Assemblage A4 is a *C. pliculosa*/*A.*

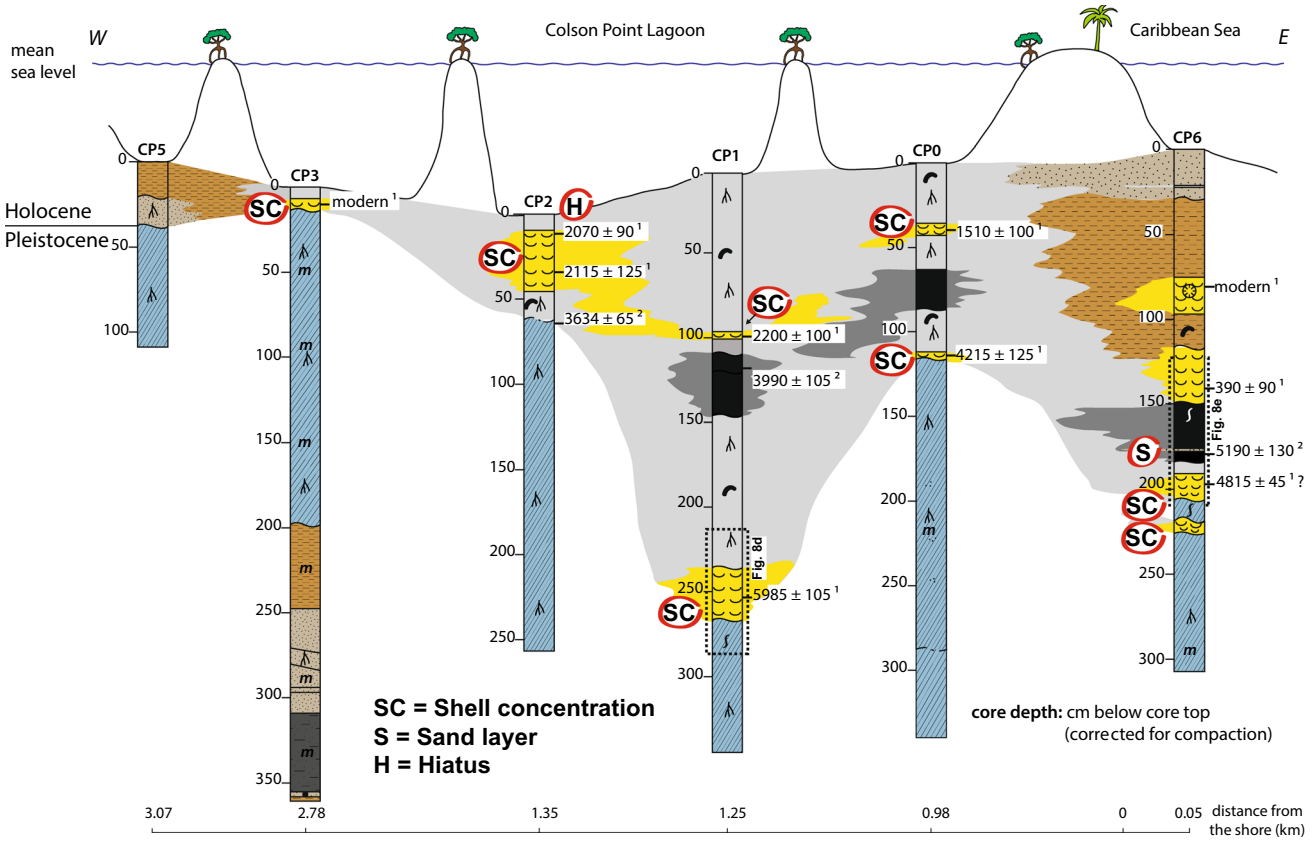

Fig. 5 Core logs and interpreted sedimentary facies at Colson Point Lagoon. Location of coring sites is shown in Fig. 2. Core logs were corrected for compaction and are arranged with reference to the sea level. Abbreviations highlight deposits, which are interpreted to be related to hurricanes. *SC* shell concentration. *Dashed rectangles* in CP1 and CP6 highlight core sections shown in Fig. 8

cuneimeris assemblage with the former being the most abundant species. Assemblage A5 is an almost monospecific assemblage, with of *C. pliculosa* and *A. cuneimeris* as dominant species. A6 comprises largely *A. cuneimeris*. A7 is an *A. cuneimeris*/*C. pliculosa* assemblage with the former being more abundant. Contacts between the shell concentrations and the under- and overlying sediments vary from sharp to gradational. The matrix of the lagoonal shell concentrations is fine-grained throughout and includes gray mud to fine sand. The shell concentration in the marginal marine core ML5, found at the base of a sand deposit close to the core top, contains marine mollusk fauna and shows a bioclast-supported fabric and a sharp contact to the underlying mud layer. One hiatus was found in core ML3 with a relatively old age of 3610 ± 90 cal yr BP close to the core top. Hiatuses are indicated by relatively old radiocarbon ages at or close to core tops. The striking age reversal in core ML2 is presumably due to diagenetic alteration of the dated mollusk shells, thereby producing a relatively young age at the base of the Holocene section.

Mullins River Beach

A distinct sand layer was found in two cores from Mullins River Beach (Figs. 4, 8b, c). It extends for at least 62 m; from core MRB1 obtained about 57 m offshore to core MRB2 collected about 5 m west of the coastline (Fig. 2b). Thickness of the sand layer decreases landward. The samples yielded radiocarbon ages of 7875 ± 85 cal yr BP in MRB1 and 7890 ± 30 cal yr BP in MRB2 (Table 4). In the remaining two cores of the transect, MRB3 and MRB4, a similar sand layer could not be identified.

The 51-cm-thick sand layer in core MRB1 was found at a corrected core depth of 232–283 cm. The medium to very coarse sand is inversely graded and its color ranges from light olive brown to yellowish brown. Like the grain size, the content of the most abundant mineral, quartz, increases upwards from 76 to 89 %. In contrast, the second most common mineral, microcline, decreases upwards from 19 to 4 %. No shell material was found in the sand. The contacts to the underlying and overlying deposits are sharp. The sand layer is overlain by an alternation of gray

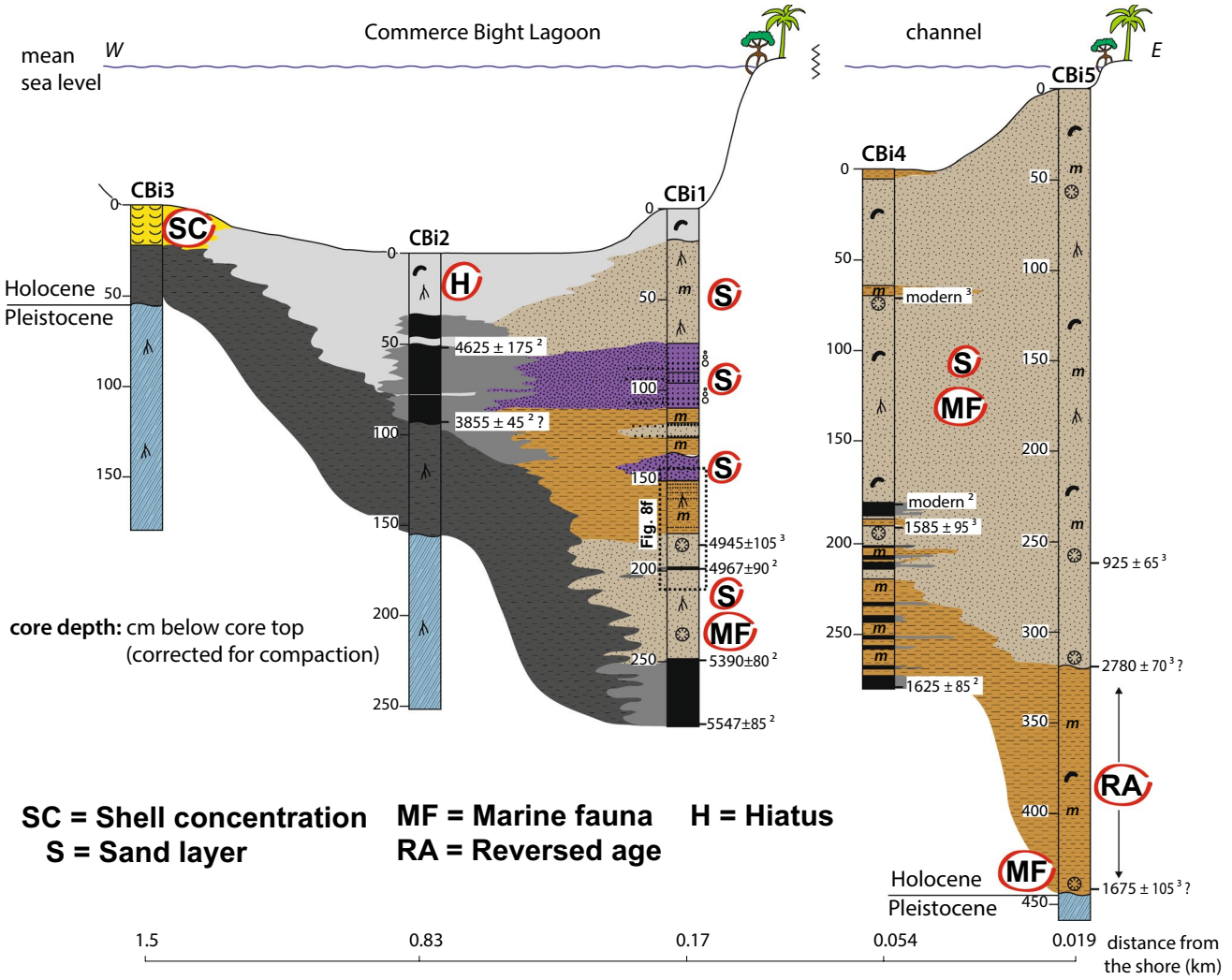

Fig. 6 Core logs and interpreted sedimentary facies at Commerce Bight Lagoon. Location of coring sites is shown in Fig. 2. Core logs were corrected for compaction and are arranged with reference to the sea level. Abbreviations highlight deposits, which are interpreted to be related to hurricanes. *SC* shell concentration, *S* sand, *MF* marine fauna, *RA* reversed age. *Dashed rectangle* in CBi1 highlights core section shown in Fig. 8

mud and silt of about 120 cm thickness. The lamination in the lower 27 cm of this deposit is regularly spaced; further upcore the lamination is less regularly spaced.

The 1-cm-thick sand layer in core MRB2 was found at a corrected core depth of 394 to 395 cm and consists of light yellowish brown medium to coarse sand. The quartz and microcline content of the sand layer is 53 and 9 %, respectively. Furthermore, this sand shows an andalusite content of 34 %, which is high compared with beach sands at the core top with less than 3 % andalusite and an andalusite content of the same-aged sand layer in core MRB1 of less than 6 %. The sand layer also lacks shells. Both contacts, to the underlying organic-rich gray mud to silt and to the overlying gray mud, are sharp. The overlying mud contains a 2-cm-thick silt layer. This deposit is similar to a deposit overlying the sand layer in core MRB1. In core MRB2, the planar laminated unit of gray mud and silt is about 41 cm thick and thus, like the sand layer, this deposit also shows landward thinning. It is overlain by another sand layer, a 65-cm-thick micaceous silt to fine sand deposit, which shows a sharp but wavy lower contact and gradually merges into laminated fine-grained sediments. The lower portion of this micaceous silt to fine sand contains rip-up clasts from the underlying gray mud (Fig. 8b). The micas observed in these deposits are flaky and have larger grain sizes than the surrounding components.

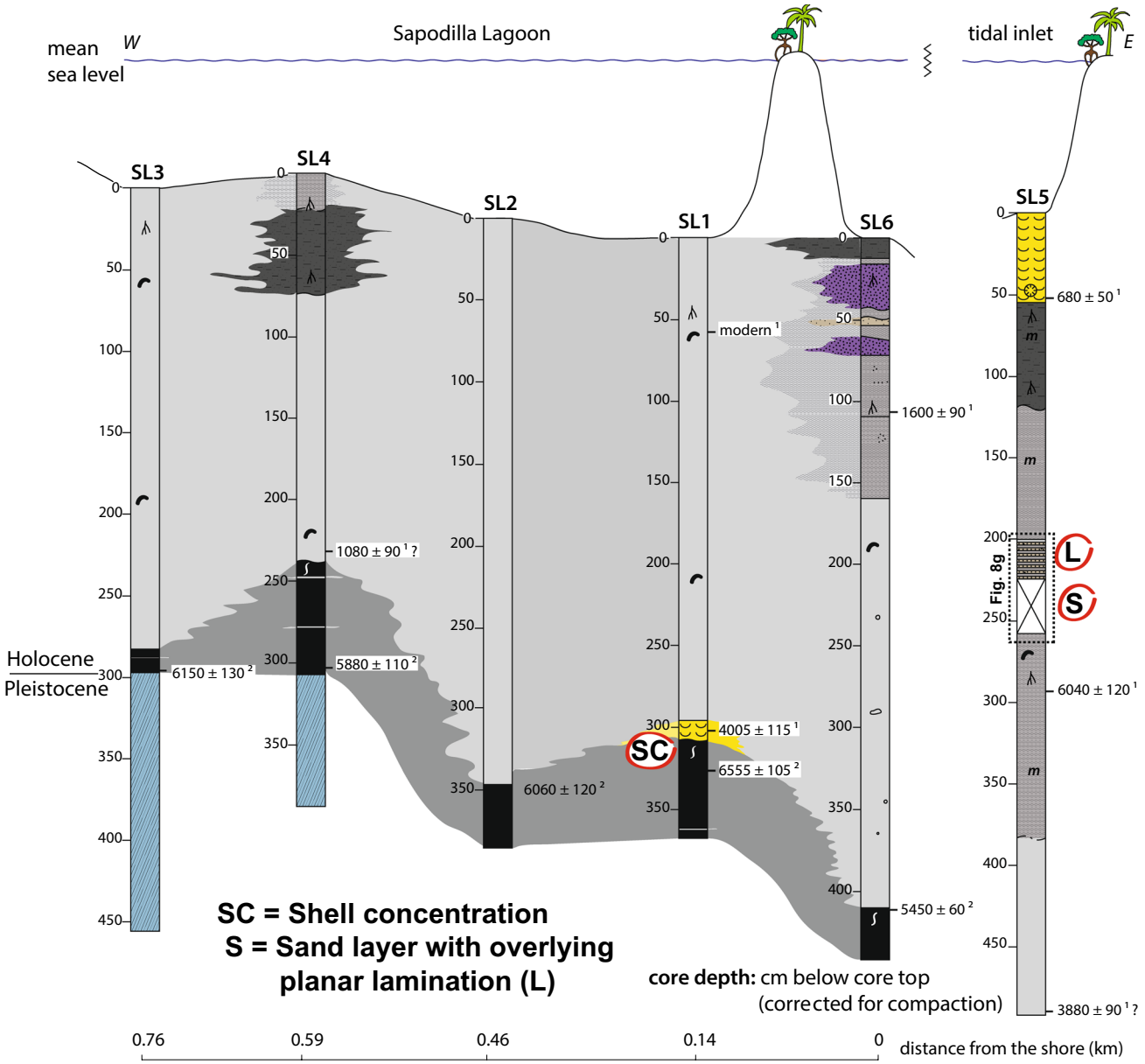

Fig. 7 Core logs and interpreted sedimentary facies at Sapodilla Lagoon. Location of coring sites is shown in Fig. 2. Core logs were corrected for compaction and are arranged with reference to the sea level. Abbreviations highlight deposits, which are interpreted to be related to hurricanes. *SC* shell concentration, *S* sand, *L* lamination. *Dashed rectangle* in SL5 highlights core section shown in Fig. 8

Colson Point Lagoon

As in Manatee Lagoon, shell concentrations are common in cores from Colson Point Lagoon. Ten shell concentrations were observed in the cores CP0, CP1, CP2, CP3 and CP6, of which eight have been interpreted as possible storm deposits (Figs. 5, 8d). Faunal composition is similar to that of the lagoonal concentrations in Manatee Lagoon. The two basal shell concentrations in core CP6, which was collected in the marginal marine area, have probably been deposited in a lagoon environment (Adomat et al. 2016). These two shell concentrations in core CP6 are graded. In contrast to the basal concentrations, the two shell concentrations further upcore represent marginal marine deposits. In core CP2, a hiatus was found, showing an age of 2070 ± 90 cal yr BP close to core top. In core CP6 from the marginal marine area east of Colson Point, a sand layer of 3 cm thickness is interbedded with mangrove peat (Fig. 8e).

Table 4 Characteristics and radiocarbon dates of possible overwash deposits including sand layers, marine fauna, hiatuses and reversed ages

Core	Corrected thickness (cm)	Type	Sediment	Lower contact	Upper contact	Sediment structures
MRB1	51	Sand layer	Medium to very coarse sand	Sharp, planar	Sharp, planar	Inverse grading, landward thinning, overlain by laminated fine-grained sediments
MRB2	1	Sand layer	Medium to coarse sand	Sharp, planar	Sharp, planar	Landward thinning, overlain by laminated fine-grained sediments
MRB2	27	Sand layer	Silt to fine sand	Sharp, wavy	Gradational	Rip-up clasts at base, micaceous, overlain by laminated fine-grained sediments
CP6	3	Sand layer	Medium to coarse sand	Sharp, planar	Sharp, planar	Sandwiched between mangrove peat
SL5	32	Sand layer	Fine sand	Sharp, wavy[a]	Sharp, planar[a]	Overlain by laminated fine-grained sediments
CBi1	248	Marine fauna	Coral fragments, coarse to very coarse sand	Gradational	Gradational	Overlying sands partially normally graded
CBi4	11	Marine fauna	Coral fragments, brackish to marine mollusks, coarse to very coarse sand	Gradational	Gradational	None
CBi5	447	Marine fauna	Coral fragments, marine mollusks, coarse to very coarse sand	Gradational	Gradational	None
ML3	0–21	Hiatus	Mud overlying shell conc.	Gradational	None	None
CP2	0–11	Hiatus	Mud overlying shell conc.	Gradational	None	None
CBi2	0–52	Hiatus	Mud overlying muddy peat	Gradational	None	None
CBi5	323–438	Reversed age	Change from silt to fine sand to medium to coarse sand	Sharp, wavy	Gradational	None

Core	Dated material	Conventional age (yr BP)	Calibrated age (cal yr BP, 2 σ range)	Calibrated age (cal yr BP)	BETA no.
MRB1	Organic matter of underlying organic mud	7050 ± 40	7960–7790	7875 ± 85	345343
MRB2	Organic matter of underlying organic mud	6950 ± 40	7920–7900, 7860–7680	7910 ± 10, 7770 ± 90	345346
MRB2	Organic matter within sand deposit	6160 ± 30	7160–6950	7055 ± 105	345345
CP6	Underlying mangrove peat	4550 ± 30	5320–5270,5220–5220, 5180–5120,5110–5060	5295 ± 25, 5220, 5150 ± 30, 5085 ± 25	307047
SL5	No age	No age	No age	No age	No age
CBi1	Coral fragment	4850 ± 30	5050–4840	4945 ± 105	317594
CBi4	Coral fragment	2130 ± 30	1680–1490	1585 ± 95	317600
CBi5	Three coral fragments from various core depths	1. 1500 ± 30	1. 990–860	1. 925 ± 65	1. 317602
		2. 3130 ± 30	2. 2850–2710	2. 2780 ± 70	2. 317603
		3. 2220 ± 30	3. 1780–1570?	3. 1675 ± 105?	3. 317604
ML3	Bivalve shell	3820 ± 30	3700–3520	3610 ± 90	348285
CP2	Bivalve shell	2560 ± 30	2160–1980	2070 ± 90	307041
CBi2	Organic matter	4080 ± 30	4800–4760, 4690–4680, 4646–4520, 4470–4450	4780 ± 20, 4685 ± 5, 4580 ± 60, 4460 ± 10	348278
CBi5	Two coral fragments	1. 3130 ± 30	1. 2850–2710	1. 2780 ± 70	1. 317603
		2. 2220 ± 30	2. 1780–1570?	2. 1675 ± 105?	2. 317604

[a] Vague due to sediment loss

? Unreliable radiocarbon age

Table 5 Characteristics and radiocarbon dates of 16 lagoon and one marginal marine (ML5) shell concentrations

Core	Corrected thickness (cm)	Fabric	Packing	Matrix	Lower contact	Upper contact	Internal structure	Conventional age (yr BP)	Calibrated age (cal yr BP, 2 σ range)	Calibrated age (cal yr BP)	BETA no.
ML2	5	Matrix-supported	Dispersed	Gray silt to fine sand	Gradational	None	Homogeneous	118.2 ± 0.4	Modern	Modern	348283
ML2	2	Matrix-supported	Dispersed	Gray mud to fine sand	Gradational	Gradational	Homogeneous, altered	5370 ± 30	5680–5560	5620 ± 60	348284
ML2	3	Matrix-supported	Loose	Gray mud to fine sand	Sharp, wavy	Gradational	Homogeneous, altered	2050 ± 30?	1560–1380?	1470 ± 90?	325009
ML3	13	Matrix-supported	Loose	Gray mud	Gradational	Gradational	Homogeneous	3820 ± 30	3700–3520	3610 ± 90	348285
ML3	14	Matrix-supported	Loose	Gray mud	Gradational	Sharp	Mottled at base	5070 ± 30	5400–5230	5315 ± 85	325011
ML4	27	Matrix-supported	Loose to dispersed	Gray mud	Gradational	Sharp	Homogeneous	105 ± 0.3	Modern	Modern	348286
ML5	14	Bioclast-supported	Dense	Yellowish brown med. sand	Sharp	Gradational	Homogeneous	680 ± 30	280–80	180 ± 100	325012
CP0	7	Matrix-supported	Dispersed	Gray mud	Gradational	Gradational	Homogeneous	2090 ± 30	1610–1410	1510 ± 100	238280
CP0	6	Matrix-supported	Loose	Gray mud	Sharp	Gradational	Bioturbation	4270 ± 30	4340–4090	4215 ± 125	348281
CP1	5	Matrix-supported	Dispersed	Gray mud	Gradational	Gradational	Homogeneous	2650 ± 30	2300–2100	2200 ± 100	307038
CP1	24	Matrix-supported	Loose	Gray mud	Gradational	Gradational	Bioturbation	5700 ± 30	6080–5890	5985 ± 105	307040
CP2	20	Matrix-supported	Loose	Gray mud	Gradational	Gradational	Homogeneous	2580 ± 30	2240–1990	2115 ± 125	307042
CP3	5	Matrix-supported	Loose	Gray mud	Gradational	Gradational	Homogeneous	520 ± 30	Modern	Modern	307044
CP6	11.5	Matrix-supported	Loose	Gray mud	Sharp	Gradational	Grading, bioturbation	4710 ± 30	4860–4770	4815 ± 45	307048
CP6	5.5	Matrix-supported	Loose	Gray mud	Sharp	Gradational	Grading, bioturbation	No age	No age	No age	No age
CBi3	19	Matrix-supported	Loose	Gray silt to fine sand	Gradational	None	Homogeneous	No age	No age	No age	No age
SL1	8	Matrix-supported	Loose	Gray mud	Sharp	Gradational	Homogeneous	4120 ± 30	4120–3890	4005 ± 115	320754

Packing categories were determined following Kidwell and Holland (1991). Lagoon concentrations are interpreted to have been formed due to salinity changes in the lagoons related to storm events. The concentration in ML5 was probably formed during a storm event

? Unreliable radiocarbon age

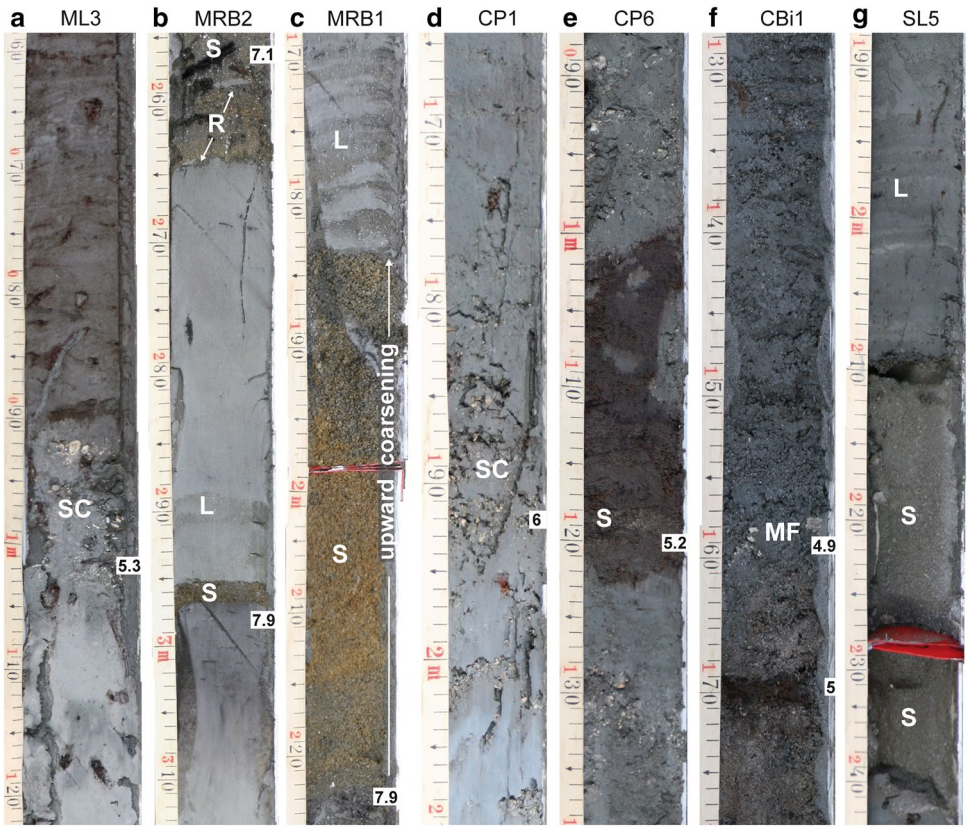

Fig. 8 Close ups of selected cores showing possible storm deposits. *Numbers* indicate rounded calibrated radiocarbon ages in kyrs BP. Note that the tape measure indicates uncorrected core depths. Location of cores is shown in Fig. 2. **a** ML3; Lagoon shell concentration (SC) overlying Pleistocene soil. **b** MRB2; Sand layer (S) with sharp contacts, overlain by laminations (L) of mud and silt. At top of the core micaceous sand layer with sharp lower contact and rip-up clasts (R). **c** MRB1; Upward coarsening sand layer (S) with sharp contacts, overlain by a planar lamination (L) of mud and silt. The thickness of the sand layer decreases landward from MRB1 to MRB2. **d** CP1; Lagoon shell concentration (SC) between Pleistocene soil and lagoonal mud. **e** CP6; Sand layer (S) in the basal portion of the mangrove peat. Bioturbation is recognizable in the upper portion of the peat and the lower lagoon shell concentration underlying the peat. Marine fauna with corals in the upper shell concentration overlying the peat. **f** CBi1; Coral fragments (MF) embedded in medium to coarse sand. **g** SL5; Sand layer (S), overlain by planar lamination (L). Fine sand was lost during cutting the core tube

Commerce Bight Lagoon

Different possible storm deposits occur in cores from Commerce Bight Lagoon (Fig. 6). At the top of the lagoonal core CBi3, a shell concentration, dominated by *A. cuneimeris* and cerithids, was found. In the lagoonal core CBi2, a hiatus with an age of 4625 ± 175 cal yr BP in 50 cm core depth was observed. The backbarrier core CBi1 shows medium to very coarse sand deposits and marine fauna that is represented by fragments of the branched coral *Porites porites*. The coral fragments and few mollusk fragments are embedded in a ca. 5-cm-thick bed within medium to very coarse sands (Fig. 8f). Underlying and overlying sediments comprise mainly quartz sands without shells and are partially graded and sporadically intercalated with fine-grained sediments. No datable material was found in these sands. One coral yielded an age of 4945 ± 105 cal yr BP (Table 4). The peat layer, which is located about 12 cm below the coral-bearing sand deposit, was dated to 4967 ± 90 cal yr BP. Only in the uppermost 20 cm of the backbarrier core, normal lagoon sediments of dark mud with brackish shells were found. *P. porites* fragments were also found in cores CBi4 and CBi5 from the tidal channel of Commerce Bight, where they occur in fine to coarse sands, together with dispersed brackish to marine and marine mollusk shells, respectively. In the lower section, core CBi5 exhibits an age reversal with older deposits overlying deposits of younger age.

Sapodilla Lagoon

At the base of Holocene sediments, the lagoonal core SL1 shows a shell concentration with abundant specimens of *A. cuneimeris* and cerithids. The shell concentration in core SL5 is not interpreted to be storm generated. Core SL5 contains a 32-cm-thick sand layer, which is overlain by

more consolidated fine-grained sediments with planar lamination (Fig. 8g). Sediment structures could not be identified due to sediment loss during cutting the core.

In summary, the following deposits have been interpreted to be related to storm events: (1) five sand layers, of which three occur in two cores from Mullins River Beach, one in a core from Colson Point and one in a core from Sapodilla Lagoon; additionally, multiple sand deposits occur in the backbarrier and in the two tidal channel cores from Commerce Bight Lagoon. (2) Marine fauna identified in sands from the lower section of the backbarrier core and from two channel cores from Commerce Bight Lagoon (3) Sixteen lagoonal shell concentrations and one marginal marine shell concentration found in eleven cores from Manatee, Colson Point, Commerce Bight and Sapodilla lagoons. (4) Three hiatuses occurring in lagoon cores from Manatee, Colson Point and Commerce Bight lagoons, and one reversed age in one core from Commerce Bight Lagoon.

Discussion

Interpretation of possible storm deposits

Sand layers

Overwash deposits in coastal lagoons are reported as grain size anomalies or sand layers in the fine-grained background sedimentation (e.g., Liu and Fearn 1993, 2000a; Lane et al. 2011). During overwash, storm surge and waves overtop the barrier crest and transport sediments landward. Overwash deposits consist of locally derived material from foredune, beach and nearshore environments and are typically well to poorly sorted fine to coarse sands (Donnelly and Webb 2004). In the study area, coarse-grained sediments are limited to the shoreface and foreshore, beach, barriers, barrier islands and barrier spits, whereas fine-grained facies were deposited in lagoon basins, tidal flats and marsh areas (Adomat and Gischler 2015). Thus, we interpret the sand layers in cores MRB1, MRB2, CP6, SL5 to have been deposited during high-energy events. At the Mullins River Beach location, the beach separates the marsh environment from the sea. There is no evidence for the existence of a barrier or beach during time of deposition of the sand layer, but the geomorphological setting of this site has changed in the past. The absence of mollusk shells in the muddy sediments, compared with muds from the other locations, suggest that a lagoon did not develop during the Holocene. Rather, a salt marsh or reed swamp environment persisted at this location (Adomat and Gischler 2015). Due to retrogradation of facies during Holocene sea-level rise, which is indicated by marine shells overlying lagoon shells in core CP6, it can be assumed that at Colson Point, the barrier had a more seaward position in the past, and at Mullins River Beach, a beach existed further seaward during early stages of coastal development. The barrier and the beach probably served as source for washover sands. At site SL5, the sand spit may have served as source for washover sands. More radiocarbon ages would be necessary to clarify whether or not the spit already existed during the time of deposition of the sand layer. Some sand deposits in the cores have not been interpreted as storm deposits, because they lack typical textural and compositional indications. Deposition of coarse-grained layers may be explained by other mechanisms such as riverine floods, eolian processes, sediment winnowing and tidal processes (Otvos 1999, 2002; Wallace et al. 2014). A landward retreat of barriers due to rising sea level and marine transgression may be an alternative explanation for these sand deposits.

Several diagnostic criteria suggest storm origin of the sand layers in cores MRB1, MRB2, CP6 and SL5. The gradual upward coarsening of the sand deposit in MRB1 indicates deposition during a high-energy event. Generally, upward-fining trends of hurricane overwash deposits are observed, but inverse grading was also found in some places (Morton et al. 2007; Williams 2010). Spiske and Jaffe (2009) observed normal grading during setup and inverse grading during return flow and attributed them to decelerating and accelerating flow, respectively. According to Ferm et al. (1972), transgressive backbarrier deposits are generally coarsening upward sequences. The landward fining of the sand layer from core MRB1 to core MRB2 indicates marine rather than fluvial origin (Switzer and Jones 2008, and references therein). The landward thinning of the deposit is indicative of overwash deposits (Liu and Fearn 2000a; Liu 2004), but thickness is dependent on local topography (Peters and Jaffe 2010). The unimodal but predominantly poor sorting suggests deposition during a storm event. Generally, storm deposits have a unimodal particle size distribution, whereas a bimodal (e.g., Goff et al. 2001, 2004; Switzer and Jones 2008) and polymodal (e.g., Morton et al. 2008; Spiske and Jaffe 2009) grain size distribution is considered as being indicative of tsunami deposits. Modality, however, is site and source dependent. The similar ages and the fact that thickness and grain size increase from the proximal to the distal end of the overwash fan suggest deposition of the two sand layers during the same event. A sharp contact with the underlying sediments, as observed in the sand deposits in cores MRB1, MRB2, CP6 and SL5, is another characteristic of overwash deposits (Donnelly et al. 2001a, b; Morton et al. 2007). According to Williams (2010), who used the presence of foraminifera as evidence for an offshore origin, the absence of foraminifera in sand layers does not necessarily rule out a marine origin of inshore deposits. Likewise, the lack of macrofauna

and foraminifera in the sand layers in cores MRB1, MRB2, CP6 and SL5 also does not exclude a storm origin of the deposits. The recent beach sand at the top of core MRB2 does not contain shells either.

Rip-up clasts composed of the underlying sediment, as found in the upper sand deposit in core MRB2, are generally attributed to erosion of underlying sediment by tsunamis due to higher velocity and energy of these events (Gelfenbaum and Jaffe 2003; Switzer and Jones 2008; Morton et al. 2007) and seem to be rare in storm deposits (Jaffe et al. 2008). However, Donnelly and Webb (2004) encountered rip-up clasts at the basal contacts of backbarrier hurricane overwash deposits and assessed them as indicative of high-velocity currents.

Characteristics of both storm and tsunami deposits depend on available source material, offshore bathymetry, onshore topography and depositional environment (Kortekaas and Dawson 2007). In the study area, tsunamis that are triggered by seismic events cannot be excluded due to the nearby active Caribbean–North American plate boundary to the south. However, in the Caribbean the frequency of major earthquakes is 1–2 orders of magnitude less than that of cyclone landfalls, and of the tsunami events recorded during AD 1492–2000, only four events could be verified (Lander et al. 2002). In general, islands of the eastern Caribbean (Greater and Lesser Antilles) seem to be more frequently affected by tsunamis than the continental areas in the west (Lander et al. 2002; O´Loughlin and Lander 2003). Tsunami deposits have been reported from many regions including the wider Caribbean, Australia and the Mediterranean (e.g., Lander et al. 2002; Scheffers and Kelletat 2003; Kelletat et al. 2004; Dominey-Howes et al. 2006; Scheffers 2006; Switzer and Jones 2008). However, Morton et al. (2008) and Spiske et al. (2008) have questioned several published Caribbean examples of tsunami deposits and reinterpreted them as storm features. Several diagnostic criteria for the distinction of storm and tsunami deposits have been proposed (e.g., Scheffers and Kelletat 2003; Morton et al. 2007; Switzer and Jones 2008), but many signatures are applicable to both storm and tsunami deposits (Switzer and Jones 2008).

Lamination of sediment was described as common diagnostic criterion for storm deposits and occurs as planar stratification with thin, often graded laminae and laminasets, or as foreset bedding (Schwartz 1975; Morton et al. 2007; Switzer and Jones 2008). The laminated sediments overlying sand layers as observed in cores MRB1, MRB2 and SL5 (Fig. 8b, c, g) are interpreted to be associated with storm events. Only one of the five sand layers in the cores, core CP6, lacks overlying laminated sediments, due to deposition in mangrove peat (Fig. 8e). The recurring stratigraphy of a sand layer with overlying laminated sediments probably reflects hydrodynamic inundation characteristics of a storm surge. In contrast to tsunamis, storms are limited only to unidirectional landward flow. However, Spiske and Jaffe (2009) described a complete hurricane surge sequence from a carbonate environment of Bonaire, the Netherlands Antilles, which shows bidirectional storm directions and consists of three sedimentary units corresponding to setup, peak and return flow of the storm surge. Storm-induced sediment deposition takes place under primarily laminar flow conditions, during a period of hours to days (Tuttle et al. 2004). According to Morton et al. (2007), the absence of mud in most sandy storm deposits is the result of persistent high-velocity and nearly unidirectional flow during the storm. Fine-grained sediments in storm deposits result from late-stage deposition from suspension. Williams (2010) detected two sedimentation styles in one storm surge deposit. The author distinguished a thick sand fan that was deposited by traction load and a thinner, finer and more organic-rich blanket that was deposited from suspension. Laminasets of alternating coarse and fine textures are indicative of high-frequency waves (Morton et al. 2007) and thin graded laminae are reported to be the result of individual waves during storm deposition (e.g., Sedgwick and Davis 2003; Switzer and Jones 2008). Laminations may be destroyed by bioturbation (Hennessy and Zarillo 1987). Due to their flaky shape, micas that occur within the laminated deposits may be easily suspended and transported in water and successively settled from suspension (Jagodziński et al. 2009). Jagodziński et al. (2009) detected abundant mica flakes in the uppermost portion of a tsunami deposit, which probably have been transported by suspension. The authors explained their absence in the lower part of the deposit by bedload transport. Several inundation pulses during storms (sensu Switzer and Jones 2008) can be regarded as possible cause for the deposition of sand layers and overlying laminated sediments encountered during this study. Generally, the thickness of sandy tsunami deposits rarely exceeds 25 cm, whereas sandy storm deposits can be up to 10 times thicker (Morton et al. 2007; Bryant 2008).

Marine fauna

The coral fragments in core CBi1 indicate a marine source and are interpreted as overwash deposits. The medium to very coarse sands found in the core probably were also transported during overwash processes. Sedimentation of coarse sands with corals and dispersed marine mollusk shells in cores CBi4 and CBi5 also results from barrier overwash. The narrow sandy barrier is situated about 100 m from CBi1. Distance from coring sites CBi4 and CBi5 to the barrier is 55 m and 20 m, respectively. Interfingering of muddy and sandy deposits indicates that lagoon background sedimentation was repeatedly interrupted by overwash. Channel migration may also explain the presence of

sand layers. However, the wavy outline at the leeward side of the sandy barrier suggests that overwash is a common process in Commerce Bight Lagoon. Sedimentation of mud with brackish shells at the top of the core demonstrates a return to lagoonal conditions. According to Hippensteel (2010), overwash deposits are the product of reworking, and therefore, dates obtained from fossils of those deposits may represent the age of the fossils but not the time of storm deposition. Morton et al. (2008) also considered problems concerning the dating of specific events because there can be substantial time elapsed between the death of an organism and the incorporation of its skeletal material into the sediment. Hence, the ages of the corals obtained do not necessarily reflect the ages of the storm events, particularly if they are not supported by other proxies. However, the radiocarbon age of the coral found in CBi1 seems to be a fairly reliable datum of overwash, because the age of the underlying peat was dated to be 20 years younger.

Shell concentrations

The accumulation of shells in the lagoons may have different origins: (1) deposition of shells by overwash during high storm surges, (2) formation of storm lags as a product of sediment winnowing during storms and subsequent accumulation of shells and (3) thriving of tolerant mollusk species due to changes in environmental conditions.

If the shells had accumulated during overwash events, both nearshore and marine mollusk species would be expected in the deposit. Overwash of marine species, mainly microfossils, into lagoons and lakes during storms is common (e.g., Hippensteel and Martin 1999; Morton et al. 2007; Hippensteel 2011; Pilarczyk and Reinhardt 2011; Hippensteel and Garcia 2014). However, the dominant species in the shell concentrations, *A. cuneimeris*, is known to tolerate a wide range of salinities. Turney and Perkins (1972) reported a salinity range of 13–80 ‰ in which living *A. cuneimeris* were found. *A. cuneimeris* lives in both enclosed and open hypersaline lagoons (Andrews 1935; Parker 1959). In Florida Bay, *A. cuneimeris* is restricted to the Northern Subenvironment, defined by only one species, which is greatly affected by freshwater drainage from the mainland (Turney and Perkins 1972). In Belize, taxonomic analysis including composition and diversity of mollusk species shows differences between the lagoonal shell concentrations and shell concentrations from the marginal marine area. Taphonomic analysis of *A. cuneimeris*, such as numbers of left and right valves (LR ratio) and size-frequency diagrams, suggests parautochthonous life assemblages, which have not been transported over wide distances and which have been deposited in their original brackish habitat. These observations indicate that the shells have not been deposited during overwash processes, and a marine origin can be excluded.

The second hypothesis is also invalid because the matrix of the shell concentrations is fine-grained and similar to lagoon background sediments. Storm lags typically lack fine matrix and have erosive bases (Brenner and Davies 1973). Only some contacts are sharp, and changes in composition between the underlying deposits and the shell concentrations were not found except for under- and overlying peats and soils. Furthermore, no taphonomic features that would reflect storm events, such as preferred orientation of valves, bioclast-supported fabric and dense packing, were observed in the shell concentrations. Grading in two shell concentrations is attributed to bioturbation. Separate dating of several shells from one shell concentration would help to elucidate time averaging within the accumulation.

Since the shells are parautochthonous, they are interpreted to have accumulated episodically in the lagoons, probably during periods of favorable environmental conditions. Episodic favorable conditions may have resulted from increased river drainage associated with storm landfall precipitation events lowering salinity. Alternatively, an increase in salinity due to marine inundation and low air pressure associated with storm surges is possible. High water levels inshore of the barriers after storms can be caused either by floodwater runoff from the mainland or remnants of the storm surge (Morton 2002). Generally, an increase in salinity as a result of inundation is postulated (Li et al. 2009). According to Liu (2004), a hurricane-induced storm surge can cause saltwater intrusion into low-salinity lakes, thereby producing abundance peaks of marine microfossils such as foraminifera, dinoflagellates and diatoms, even without significant overwash deposition (Li 1994; Hemphill-Haley 1996; Zhou 1998; Collins et al. 1999; Hippensteel and Martin 1999; Liu et al. 2003). But the contrary has also been demonstrated. Hoese (1960) showed that heavy rainfall after drought led to a rapid decrease in salinity of more than 30 ‰, causing a mortality of stenohaline mollusks in the bay fauna of Mesquite Bay on the central Texas coast. A decrease in salinity after landfall of a hurricane was reported from a brackish water coastal backbarrier lake separated from the Gulf of Mexico and related to freshwater input from surrounding marsh area as a result of heavy rain (Liu et al. 2011). Changes in environmental conditions are probably related to changes in geomorphology during Holocene evolution of the lagoons, i.e., the formation of barriers and spits. Unfavorable conditions that allowed tolerant species such as *A. cuneimeris* and cerithids to flourish may have promoted the formation of shell concentrations. Storm events may have caused environmental variation such as salinity changes. In an area with highly variable precipitation such as in Belize, heavy rainy season or rain

events during a dry season are to be considered as alternative explanations for environmental changes. The record by McCloskey and Liu (2012) from Belize also exhibits a dual sensitivity to both wind and rain. The authors considered both seaward and landward input and discussed the link between hurricane activity and strong precipitation events. Profiles of terrestrial elements such as Fe, Ti, Cr, Mn, Zn and Ti and marine elements such as S, Cl and Br served as environmental proxies and helped the authors to distinguish between inland and seaward origin of sediments. In contrast to the lagoonal shell concentrations, which are considered to represent indirect evidence of storm events, the concentration together with the overlying sand deposit in the marginal marine core ML5 may represent direct evidence of storm deposition. This is suggested by its position at the base of the sand deposit, the densely packed, bioclast-supported nature and the sharp contact to the underlying mud layer. Origin of the shell concentration at the top of core SL5 from the tidal inlet to Sapodilla Lagoon is probably not storm related but rather formed due to higher energy in the tidal channel and the presence of a more diverse fauna related with mangrove vegetation.

Hiatuses and age reversals

The relatively old radiocarbon ages at or close to core tops, as observed in three cores from Manatee, Colson Point and Commerce Bight Lagoons, suggest erosion during high-energy events. McCloskey and Liu (2012) also recognized relatively old ages at top of cores from Commerce Bight Lagoon and interpreted them as the results of storm-induced erosion.

Age reversals, as observed in six cores from Mullins River Beach (MRB3) and Manatee, Colson Point, Commerce Bight and Sapodilla Lagoons (ML2, CP6, CBi2, CBi5 and SL5), also may indicate storm influence. However, only the age reversal in core CBi5 is interpreted to be storm influenced, since the dated corals are likely redeposited and further indications for storms such as coarse sands occur in the core. In the other five cores, age reversal is possibly due to diagenetic alteration of dated material, young root penetration from above and bioturbation. Erosion and sediment mixing resulting in reversed ages may also be caused by other processes, such as river floods or tsunamis. However, in the study area a storm origin is quite likely. Limitations in radiocarbon dating may also be a conceivable explanation for reversed ages. Dated bivalve shell material may have undergone diagenetic alteration, which resulted in reversed ages as observed in cores ML2 and SL5. Radiocarbon dating of organic matter from peats and peaty sediments may produce too young ages due to contamination by younger roots. This could explain the reversed ages in core CBi2. The relatively old date in MRB3 may be attributed to the charred nature of the dated organic material, resulting in a too old age. Bioturbation processes, which are indicated by reworking of sediment, wavy lower contacts and grading of shells, probably caused the reversed age in core CP6.

Comparison with other studies

In this study, some thirty potential event beds have been identified along the central Belize coast during a time

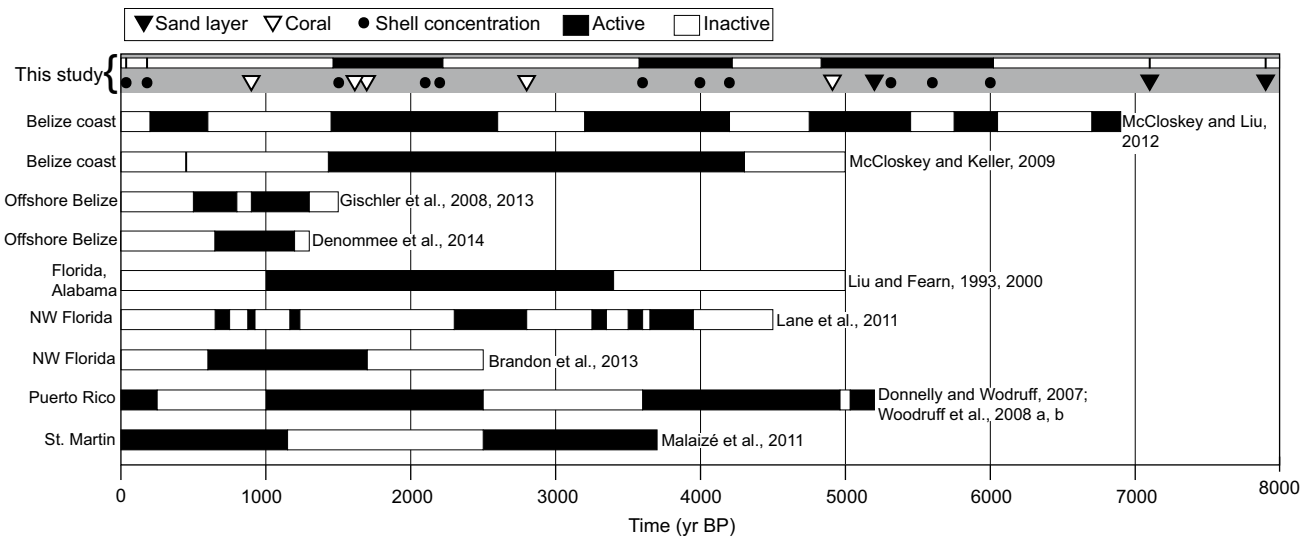

Fig. 9 Ages of possible event deposits identified in the study area, compared with paleohurricane records from the Belize coast, offshore Belize, the Gulf Coast and the Antilles archipelago. Three periods with event deposits being more frequent can be recognized. Ages of different proxies, including sand layers, shell concentrations and corals, are shown in the diagram. Coral ages were only included if supported by other proxies as there is a possibility that they are older than the surrounding sediment

interval of 8 kyrs (Tables 4, 5). Sand layers, shell concentrations and marine fauna, represented by corals, are interpreted as storm event beds and included in the diagram on Fig. 9. Due to the fact that ^{14}C-ages from corals might be considerably older than the event deposits in which they occur, ages not supported by additional evidence have not been interpreted as being related to hurricane activity. Hiatuses, age reversals and the unreliable age of the shell concentration in ML2 are not figured because they exhibit a wide range of the ages and ages do not obligatorily indicate the time of hurricane landfall. A number of event deposits can be grouped into three phases occurring from 6000 to 4900, from 4200 to 3600 and from 2200 to 1500 cal yr BP. In addition, there are two earlier events positioned around 7900 and 7100 cal yr BP and more recent events centered around 180 cal yr BP and during modern times (Fig. 9). The fact that 5 major hurricanes have been recorded in the study area during the past 150 years but only one storm deposit during 250- to 300-year periods on average during the studied time interval of the past 8 kyrs clearly suggests incompleteness of the record. However, it is the best storm record there is from the studied interval in the area. The clustering of events during certain time periods furthermore allows to approximately contrast active and inactive storm intervals, thereby permitting comparisons with other paleotempestology studies. It has to be kept in mind, however, that determination of active and inactive periods based on the identified event deposits is debatable due to the low number of event deposits, the use of different proxies and the fact that the event deposits originate from several sites along the coast.

A comparison with storm activity data from other studies shows both coincidences and differences (Fig. 9). Identified storm events match best with data from McCloskey and Liu (2012) from south-central Belize. Furthermore, some temporal correlations with hurricane activity periods from Puerto Rico (Donnelly and Woodruff 2007; Woodruff et al. 2008a, b) exist. The hurricane frequency records from the Gulf of Mexico and the Antilles archipelago exhibit differences to the Belize records (Fig. 9). The comparison with the shorter high-resolution storm records from offshore Belize of Gischler et al. (2008, 2013) and Denommee et al. (2014) shows that correlation between storm layers, even in one region, is difficult. However, small discrepancies even exist between these two offshore records.

Along the Belize coast, McCloskey and Keller (2009) obtained 15 cores with a maximum length of ca. 2.4 m from the coastal area about 1 km south of our study site, and six cores from Gales Point, about 3.7 km north of our study site. They interpreted interbedded sand and clay layers as storm deposits, correlated these to hurricane events and identified a period of clustered hurricane events ranging from 4500 to 2500 yr BP and one extreme event around 450 yr BP. McCloskey and Liu (2012) studied a transect of seven cores with a maximum core length of 3.1 m from the eastern area of Commerce Bight Lagoon. After ca. 2000 yr BP, a change from a wetland to a lake environment occurred, according to these authors. They interpreted clastic layers of sand as storm deposits, being generated by storm surges and storm-induced precipitation events, and distinguished between active and quiet periods, lasting from several centuries to 1200 years. Within the 7000-year record, they identified six active periods: 6900–6700 yr BP, 6050–5750, 5450–4750, 4200–3200, 2600–1450 and 600–200 yr BP. High-resolution data for the last 1500 years from the Belize Blue Hole sinkhole, located on the Lighthouse Reef Atoll, suggest intense hurricane activity from 500 to 800 yr BP, from 900 to 1300 yr BP (Gischler et al. 2008, 2013) and from 650 yr BP to 1200 yr BP (Denommee et al. 2014). Deviations between the two records are based on the fact that different minimal grain sizes have been used to define event layers, which resulted in different numbers of storm deposits.

Further studies from the Gulf Coast and the Caribbean have documented hurricane activity spanning the last 7000 years. As proxy for the paleohurricane reconstructions, coarser grained deposits in fine-grained background sediments have been used. Lane et al. (2011) detected grain size anomalies in sediments from a coastal sinkhole at Apalachee Bay, NW Florida, and constructed both low and high threshold event chronologies with seven intervals in the high threshold series that exhibit event frequencies at or above three events per century. Brandon et al. (2013) yielded a period of increased intense hurricane frequency between 1700 and 600 yr BP from an adjacent area at Appalachee Bay. Sand layers in coastal lake and marsh sediments from Alabama and NW Florida indicate a hyperactive phase from 3400 to 1000 yr BP and quiescent phases from 5000 to 3400 yr BP and from 1000 yr BP to present (Liu and Fearn 1993, 2000a, b). However, the records by Liu and Fearn (1993, 2000a, b) have been intensively criticized by Otvos (1999, 2002). According to this author, most of the sand laminae, which have been related to overwash during catastrophic hurricanes by Liu and Fearn (1993, 2000a, b), have accumulated in a valley-filled estuary. As Otvos (1999) noted, other sedimentary processes than storm-surge overwash may have served as sand sources. Furthermore, Otvos (1999, 2001, 2002) questioned the radiocarbon dates of Liu and Fearn (1993) and criticized that Liu and Fearn (2000a, b) treated the barrier as fixed although coastal barriers are dynamic systems and the sensitivity of a site to overwash may have changed over time. The record of intense hurricane activity established by Donnelly and Woodruff (2007) and Woodruff et al. (2008a, b) in Puerto Rican lagoons demonstrates intervals of relatively frequent intense hurricane strikes from 5400 to

3600 yr BP, from 2500 to 1000 yr BP and from 250 yr BP to present. Fewer intense strikes have been recorded around 5000 yr BP, between 3600 and 2500 yr BP and between 1000 and 250 yr BP. Malaizé et al. (2011) investigated lacustrine pond sediments from Saint Martin (northern part of Lesser Antilles archipelago) and identified two relatively dry climatic periods from 3700 to 2500 yr BP and from 1150 yr BP to the present with predominantly carbonate mud deposition, droughts and hurricane events. In contrast, during a humid period from 2500 to 1150 yr BP, deposition of black organic mud occurred during pond highstand.

In the studied region, Holocene climate variability in the region is characterized by a change from warmer/wetter conditions during the Holocene Climate Optimum (ca. 10000–5500 yrs BP) to cooler/drier conditions after ca. 5000 yrs BP (e.g., Haug et al. 2001). Another change back to warmer and wetter conditions occurred in the late Holocene (between 3000 and 1000 yrs BP) in the wider study area according to vegetation data (Wooller et al. 2009) and coral climate proxy data from Belize (Gischler and Storz 2009). A period of increased hurricane activity during 3500–1000 yrs BP recorded by Liu and Fearn (2000a, b) apparently correlated with a northward shift of the Intertropical Convergence Zone (ITCZ). A northern position of the ITCZ favors heavy rainfall in the southern part of the Caribbean and the Yucatán peninsula, whereas a southern position of the ITCZ causes drought in the Caribbean region (Haug et al. 2003; Hodell et al. 2005). Stronger storm activity over the Gulf coast and the inner Caribbean Sea is favored by a southern position of the ITCZ in connection with dry climatic conditions. The position of the ITCZ is associated with a shift of the Bermuda High, whose position controls the direction of hurricane paths. Therefore, differences in hurricane frequency can be observed in the Caribbean as shown in the records in Fig. 9. Data from localities positioned in the same region such as Puerto Rico and St. Martin or coastal lagoons and offshore sinkholes in Belize also differ, suggesting that the preservation of hurricane deposits plays an important role as well.

Suitability of Belize barrier–lagoon complexes for reconstruction of storm events

The preservation potential of sandy storm deposits appears to be higher in beach and marginal marine settings than in coastal lagoons. The cores investigated during this study that contain sandy storm deposits derive from the beach (core MRB2), the marginal marine area (cores MRB1 and CP6) and the tidal inlet (core SL5) (Fig. 2). Core CBi1 is the only core from a lagoonal basin that contains washover sands, which is attributed to the adjacency to the barrier. Along the Belize coast, which has been hit by hurricanes on a regular basis, a higher number of overwash deposits in lagoons may be expected. Still, in the cores that contain sand layers, the storm record is poor when considering the frequency of historical hurricane landfalls. Liu (2004) stated that in coastal lake sites, which are repeatedly impacted by landfalling hurricanes, sediment cores are expected to contain multiple layers of overwash deposits sandwiched between normal organic lake sediments. The fact that cores taken from the central lagoon basin do not contain washovers may be attributed to several factors. According to Sedgwick and Davis (2003), the preservation potential of individual storm deposits is highly variable and depends on factors such as the rate of bioturbation, frequency of overwash, thickness of the units as well as the magnitude and rate of sea-level change. Liu (2004) noted that the preservation potential of sediments deposited at the bottom of coastal lakes, which are isolated from the sea, is higher than in shallow-water marine environments, because overwash deposits will not be removed by tidal scouring or reworking. According to this author, shallow marine environments are inappropriate for providing high-resolution records because of reworking and obliteration by subsequent storm events. The relatively poor record in the Belize lagoon cores may result from biological and physical processes in the lagoons. Bioturbation is a common process in the lagoons, and evidence of bioturbation was also found in several cores (Fig. 8e). In mangrove-vegetated environments, the benthic fauna is typically dominated by burrowing decapods such as crabs (Kristensen 2008). They dig and maintain burrows in the sediment, affecting sediment topography by physical displacement of particles. The burrowing activity may destroy sediment structures and hampers the identification of event deposits. Erosion of sands by tidal flushing is limited because the Belize coast is a microtidal area with a tidal range of max. 30 cm. The coastal lagoons in the study area are tidally connected to the sea. However, they represent restricted, not open lagoons (Fig. 2). Manatee, Colson Point and Commerce Bight lagoons are connected with the sea by relatively long bifurcating and branched tidal channels. An exception is Sapodilla Lagoon, which is less restricted than the other lagoons. Here, the permanent broad tidal inlet, which is interpreted to have been formed by spit progradation (Adomat and Gischler 2015), and the channel between the narrow spit and the barrier island allow water exchange with the open ocean. The core sites of MRB1, CP6 and SL5, which contain event sand layers, are today located in areas with increased water energy, compared with the lagoon basins. But during time of deposition of the sand layers, low water energy prevailed at the sites, which is supported by the predominant fine-grained sediments in the cores.

In addition to bioturbation and tidal flushing, some other aspects need to be considered, which may reduce the fidelity of the sediment archive: After two or more events that

occurred in a relative short time interval, the lack of enough material for erosion and deposition may cause that no depositional evidence was left in the record after an event. Furthermore, event beds that have been deposited back-to-back may not be registered as separate events. The top of the first event bed may not be covered by background sediments and thus is vulnerable to erosion. During deposition of the subsequent event bed, partial removal of the top of the earlier event deposit may occur, producing amalgamated event beds, as observed by Keen et al. (2004) and McCloskey and Keller (2009). Not all variations in faunal composition may be preserved in the record. Evidences of minor changes in faunal composition that occur in the time period until the conditions return to the initial level (e.g., until the barrier got reestablished) may not be registered in the record. Hence, it has to be taken into account for how long the conditions such as barrier breaching or freshwater input that caused the variations prevailed.

Besides the reduction in the preservation potential, the occurrence of storm deposits is also dependent on the sensitivity of a site to storm deposition (Hippensteel et al. 2013). The paleotempestological sensitivity of a lake or lagoon, which is enclosed by a barrier, in turn depends on meteorological factors, long-term changes in sea level and geomorphological factors (Liu 2004). These factors may have changed over time and thus also the sensitivity may have changed over time. Sea-level rise may have a strong influence on site sensitivity, especially on low-lying coastal areas as in Belize. Only intense storms produce high storm surges that are able to overtop the barrier. Sand deposition is also possible during less intense storms via active channels and inlets (Donnelly et al. 2001a). Geomorphological factors such as offshore bottom slope, coastline configuration, supply of floodwater from river discharge as well as stochastic meteorological factors influence the relationship between storm surge height and hurricane intensity (Jarvinen and Neumann 1985; Hubbert and McInnes 1999). Whether a storm surge will overtop a barrier depends primarily on two factors, the storm surge height and the barrier height (Liu 2004). Storm surges of weaker hurricanes possibly were not able to exceed the barrier. According to Malaizé et al. (2011), only high-intensity hurricanes significantly contribute to event sedimentation. Most sites only record hurricanes that make landfall in the immediate vicinity at major hurricane strength (category 3 or above) (Donnelly and Webb 2004; Liu 2004; Elsner et al. 2008; McCloskey and Keller 2009; McCloskey and Liu 2012). According to Morton et al. (2007), the highest storm surges of tropical cyclones are generally restricted to a few tens of kilometers adjacent to the eye, although elevated water levels can encompass more than 600 km of coast. The characteristics of hurricanes lead to different hurricane effects of the two sides of the storm track. Vortex winds flow counterclockwise around the eye, and much slower regional winds move the storm system forward. On the right side of a hurricane, the winds are stronger, because the two winds move in the same direction and are additive (Coch 1994). Thus, low correlation of event beds from the study area to published records from areas in greater distance from the study area is not surprising.

Mangrove vegetation, which densely fringes the coastal lagoons in the study area since ca. 6 kyrs BP, acts as a protective barrier against erosion during storm or flood events (e.g., Danielsen et al. 2005; Kathiresan and Rajendran 2005), tends to reduce the magnitude of erosion (Morton 2002) and may also prevent a complete storm record. Mangroves are able to attenuate storm surges by reducing the surge amplitude and by reducing the inundation distances (e.g., Zhang et al. 2012; Liu et al. 2013). It has been shown that mangroves are more effective at reducing surges from hurricanes with a rapid forward speed than those of hurricanes with a slow forward speed (Zhang et al. 2012). Because of their dense stilt roots, trees of *R. mangle* are effective in dissipating the energy of low surges (McIvor et al. 2012; Zhang et al. 2012)

In summary, the following features can be regarded as favorable for paleotempestology reconstructions in the coastal lagoons: The situation behind a sandy barrier and the proximity to the sea, which is the case for Manatee and Commerce Bight Lagoons, and, with a slightly larger distance to the sea, for Colson Point Lagoon, makes the coastal lagoons susceptible to overwash. In contrast, several processes may impede reconstruction of a hurricane record: Bioturbation is a common process in the lagoons. Tidal flushing, although the coast is microtidal, plays a minor role and is strongest in Sapodilla Lagoon, where the tidal inlet is relatively broad. Due to the connections of the coastal lagoons to major rivers, the record in coastal lagoons may be complicated by fluvial events unrelated to hurricane strikes. Sea-level rise and transgression of the sediment complexes during the Holocene may have a negative effect, because in transgressive settings storm records will be destroyed or obscured through time (Hippensteel 2010). The dynamic nature of coastal environments complicates the interpretation of sedimentary records (Donnelly et al. 2001a). Dense mangrove growth, which is found at all localities except for Mullins River Beach, is able to prevent hurricane impacts in the lagoons to some degree and thus reduces the sensitivity of the sites for overwash.

Conclusions

1. Five proxies of possible event deposits including sand layers, marine fauna represented by corals embedded in coarse sands, lagoon shell concentrations, hiatuses and age reversals could be identified in 17 cores from coastal lagoon environments in central Belize.

2. The 8000-year record allows grouping of event deposits from 6000 to 4900, from 4200 to 3600 and from 2200 to 1500 cal yr BP. Two events occurred earlier, around 7900 and 7100 cal yr BP. Further events have been dated to around 180 cal yr BP and to modern times.
3. The sand layers and corals have a marine origin and probably represent washover deposits. The shell concentrations presumably reflect periods of lowered salinity, which may have resulted from increased river discharge, associated with hurricane landfalls, or increased salinity after inundation by seawater during storms.
4. Sand layers have been observed in cores from a marsh area, the marginal marine area, the tidal inlet and the backbarrier area of a lagoon, but not in cores from the lagoon basins, suggesting a low preservation potential in the lagoons. The preservation potential of storm deposits depends on physical and biological processes such as bioturbation and tidal flushing. Additionally, deposits of severe, infrequent events are more likely to be preserved because they are thicker, contain coarser clasts and extend more landward.
5. The record displays sediments of certain events on the one hand and sediments of time spans that passed between the events on the other hand. Evidence for event deposits that have occurred within short time periods and small events that have happened between severe events may not be stored in the record due to insufficient resolution of the archive. The sensitivity of the study area to overwash deposition has changed over time due to the dynamic nature of coastal environments. There is evidence of single event deposits in coastal environments and a potential influence on the lagoon fauna due to hurricane-induced salinity changes. However, the suitability of the study area for paleohurricane reconstructions is limited, which is indicated by the scarcity of overwash deposits in lagoon basins and the moderate correlation and consistency of identified event deposits among cores and localities.

Acknowledgments We are grateful to the Deutsche Forschungsgemeinschaft (Gi222/20) and the Alfons and Gertrud Kassel-Stiftung, who funded this project. We thank Stefan Haber, Malo Jackson, David Geban and Claire Santino for help during fieldwork. Nils Prawitz, Anja Isaack and Lars Klostermann assisted during sample preparation in the home laboratory. Rainer Petschick ran the X-ray diffractometer. Michaela Spiske and an anonymous reviewer whose useful comments helped to improve the manuscript are gratefully acknowledged.

References

Adomat F, Gischler E (2015) Sedimentary patterns and evolution of coastal environments during the Holocene in central Belize, Central America. J Coast Res 31:802–826

Adomat F, Gischler E, Oschmann W (2016) Taxonomic and taphonomic signatures of mollusk shell concentrations from coastal lagoon environments in Belize, Central America. Facies 62:1–29

Andrews EA (1935) Shell repair by the snail, Neritina. J Exp Zool 70:75–107

Bender MA, Knutson TR, Tuleya RE, Sirutis JJ, Vecchi GA, Garner ST, Held IM (2010) Modeled impact of anthropogenic warming on the frequency of intense Atlantic hurricanes. Science 327:454–458

Brandon CM, Woodruff JD, Lane P, Donnelly JP (2013) Tropical cyclone wind speed constraints from resultant storm surge deposition: A 2500 year reconstruction of hurricane activity from St. Marks, FL. Geochem Geophys Geosyst 14:2993–3008

Brenner RL, Davies DK (1973) Storm-generated coquinoid sandstone: genesis of high-energy marine sediments from the Upper Jurassic of Wyoming and Montana. Geol Soc Am Bull 84:1685–1698

Bryant E (2008) Tsunami: the underrated hazard. Springer, Berlin

Coch NK (1994) Geologic effects of hurricanes. Geomorphology 10:37–63

Collins ES, Scott DB, Gayes PT (1999) Hurricane records on the South Carolina coast: can they be detected in the sediment record? Quatern Int 56:15–26

Danielsen F, Sorensen MK, Olwig MF, Selvam V, Parish F, Burgess ND, Hiraishi T, Karunagaran VM, Rasmussen MS, Hansen LB, Quarto A, Suryadiputra N (2005) The Asian tsunami: a protective role for coastal vegetation. Science 310:643

Denommee KC, Bentley SJ, Droxler AW (2014) Climatic controls on hurricane patterns: a 1200-y near-annual record from Lighthouse Reef, Belize. Sci Rep 4:3876

Dominey-Howes DTM, Humphreys GS, Hesse PP (2006) Tsunami and paleotsunami depositional signatures and their potential value in understanding the late-Holocene tsunami record. Holocene 16:1095–1107

Donnelly JP (2005) Evidence of past intense tropical cyclones from backbarrier salt pond sediments: A case study from Isla de Culebrita, Puerto Rico, USA. J Coast Res 42:201–210

Donnelly JP, Webb T (2004) Backbarrier sedimentary records of intense hurricane landfalls in the northeastern United States. In: Murnane R, Liu K (eds) Hurricanes and typhoons: past present and potential. Columbia Press, New York, pp 58–96

Donnelly JP, Woodruff JD (2007) Intense hurricane activity over the past 5,000 years controlled by El Nino and west African monsoon. Nature 447:465–468

Donnelly JP, Bryant SS, Butler J, Dowling J, Fan L, Hausmann N, Newby P, Shuman B, Stern J, Westover K, Webb T (2001a) 700 yr sedimentary record of intense hurricane landfalls in southern New England. Geol Soc Am Bull 113:714–727

Donnelly JP, Roll S, Wengren M, Butler J, Lederer R, Webb T (2001b) Sedimentary evidence of intense hurricane strikes from New Jersey. Geology 29:615–618

Donnelly JP, Butler J, Roll S, Wengren M, Webb T (2004) A backbarrier overwash record of intense storms from Brigantine, New Jersey. Mar Geol 210:107–121

Donnelly JP, Hawkes AD, Lane P, MacDonald D, Shuman BN, Toomey MR, van Hengstum PJ, Woodruff JD (2015) Climate forcing of unprecedented intense-hurricane activity in the last 2000 years. Earth's Future 3:1–17

Elsner JB, Kossin JP, Jagger TH (2008) The increasing intensity of the strongest tropical cyclones. Nature 455:92–95

Emanuel K (2005) Increasing destructiveness of tropical cyclones over the past 30 years. Nature 436:686–689

Emanuel K, Sundararajan R, Williams J (2008) Hurricanes and global warming: Results from downscaling IPCC AR4 simulations. Bull Am Meteorol Soc 89:347–367

Evan AT, Vimont DJ, Heidinger AK, Kossin JP, Bennartz R (2009) The role of aerosols in the evolution of tropical North Atlantic Ocean temperature anomalies. Science 324:778–781

Ferm JC, Milici RC, Eason JE (1972) Carboniferous depositional environments in the Cumberland Plateau of Southern Tennessee and Northern Alabama. Geological Society of America, Southeast Section, Field Guide, New York

Gelfenbaum G, Jaffe B (2003) Erosion and Sedimentation from the 17 July, 1998 Papua New Guinea Tsunami. Pure Appl Geophys 160:1969–1999

Gillett NP, Stott PA, Santer BD (2008) Attribution of cyclogenesis region sea surface temperature change to anthropogenic influence. Geophys Res Lett 35:L09707

Gischler E, Storz D (2009) High-resolution windows into Holocene climate using proxy data from Belize corals (Central America). Palaeobiodivers Palaeoenviron 89:211–221

Gischler E, Shinn EA, Oschmann W, Fiebig J, Buster NA (2008) A 1,500 year Holocene Caribbean climate archive from the Blue Hole, Lighthouse Reef, Belize. J Coast Res 24:1495–1505

Gischler E, Anselmetti FS, Shinn EA (2013) Seismic stratigraphy of the Blue Hole (Lighthouse Reef, Belize), a late Holocene climate and storm archive. Mar Geol 344:155–162

Goff JR, Chague-Goff C, Nichol S (2001) Palaeotsunami deposits: a New Zealand perspective. Sediment Geol 143:1–6

Goff JR, McFadgen BG, Chague-Goff C (2004) Sedimentary differences between the 2002 Easter storm and the 15th century Okoropunga tsunami, southeastern North Island, New Zealand. Mar Geol 204:235–250

Goldenberg SB, Landsea CW, Mestas-Nuñez AM, Gray WM (2001) The recent increase in Atlantic hurricane activity: causes and implications. Science 293:474–479

Haug GH, Hughen KA, Sigman DM, Peterson LC, Röhl U (2001) Southward migration of the intertropical convergence zone through the Holocene. Science 293:1304–1308

Haug GH, Gunther D, Peterson LC, Sigman DM, Hughen KA, Aeschlimann B (2003) Climate and the collapse of Maya civilization. Science 299:1731–1735

Hemphill-Haley E (1996) Diatoms as an aid in identifying late-Holocene tsunami deposits. Holocene 6:439–448

Hennessy JT, Zarillo GA (1987) The interrelation and distinction between flood-tidal delta and washover deposits in a transgressive barrier island. Mar Geol 78:35–56

High LR Jr (1969) Storms and sedimentary processes along the northern British Honduras coast. J Sediment Petrol 39:235–245

High LR Jr (1966) Recent coastal sediments of British Honduras. Dissertation, Rice University, Texas

High LR Jr (1975) Geomorphology and sedimentology of Holocene coastal deposits, Belize. In: Wantland KF, Pusey WC (eds) Belize shelf-carbonate sediments, clastic sediments, and ecology. AAPG Stud Geol, vol 2, pp 53–96

Hippensteel SP (2010) Paleotempestology and the pursuit of the perfect paleostorm proxy. GSA Today 20:52–53

Hippensteel SP (2011) Spatio-lateral continuity of storm overwash deposits in back barrier marshes. Geol Soc Am Bull 123:2277–2294

Hippensteel SP, Garcia WJ (2014) Micropaleontological evidence of prehistoric Hurricane Strikes from Southeastern North Carolina. J Coast Res 30:1157–1172

Hippensteel SP, Martin RE (1999) Foraminifera as indicator of overwash deposits, barrier island sediment supply, and barrier island evolution, Folly Island, South Carolina. Palaeogeogr Palaeoclimatol Palaeoecol 149:115–125

Hippensteel SP, Eastin MD, Garcia WJ (2013) The geological legacy of Hurricane Irene: implications for the fidelity of the paleostorm record. GSA Today 23:4–10

Hodell DA, Brenner M, Curtis JH (2005) Terminal Classic drought in the northern Maya Lowlands inferred from multiple sediment cores in Lake Chichancanab (Mexico). Quatern Sci Rev 24:1413–1427

Hoese HD (1960) Biotic changes in a bay associated with the end of a drought. Limnol Oceanogr 5:326–336

Holland GJ, Webster PJ (2007) Changes in tropical cyclone number, duration, and intensity in a warming environment. Philos Trans R Soc 365:454–458

Hoyos CD, Agudelo PA, Webster PJ, Curry JA (2006) Deconvolution of the factors contributing to the increase in global hurricane intensity. Science 312:94–97

Hubbert G, McInnes K (1999) A storm surge inundation model for coastal planning and impact studies. J Coast Res 15:168–185

Jaffe BE, Morton RA, Kortekaas S, Dawson AG, Smith DE, Gelfenbaum G, Foster IDL, Long D, Shi S (2008) Reply to Bridge (2008) Discussion of articles in "Sedimentary features of tsunami deposits". Sediment Geol 211:95–97

Jagodziński R, Sternal B, Szczuciński W, Lorenc S (2009) Heavy minerals in 2004 tsunami deposits on Kho Khao Island, Thailand. Pol J Environ Stud 18:103–110

Jarvinen BJ, Neumann CJ (1985) An evaluation of the SLOSH storm surge model. Bull Am Meteorol Soc 66:1408–1411

Kathiresan K, Rajendran N (2005) Coastal mangrove forests mitigated tsunami. Estuar Coast Shelf Sci 65:601–606

Keen TR, Bentley SJ, Vaughan WC, Blain CA (2004) The generation and preservation of multiple hurricane beds in the northern Gulf of Mexico. Mar Geol 210:79–105

Kelletat D, Scheffers A, Scheffers A (2004) Holocene tsunami deposits on the Bahaman islands of Long Island and Eleuthera. Z Geomorphol 48:519–540

Kidwell SM, Holland SM (1991) Field description of coarse bioclastic fabrics. Palaios 6:426–434

Kjerfve B, Ruetzler K, Kierspe GH (1982) Tides at Carrie Bow Cay, Belize. Smithson Contrib Mar Sci 12:47–52

Knutson TR, McBride JL, Chan J, Emanuel K, Holland G, Landsea C, Held I, Kossin JP, Srivastava AK, Sugi M (2010) Tropical cyclones and climate change. Nat Geosci 3:157–163

Kortekaas S, Dawson AG (2007) Distinguishing tsunami and storm deposits: an example from Martinhal, SW Portugal. Sed Geol 200:208–221

Kristensen E (2008) Mangrove crabs as ecosystem engineers; with emphasis on sediment processes. J Sea Res 59:30–43

Lander JF, Whiteside LS, Lockridge PA (2002) A brief history of tsunamis in the Caribbean Sea. Sci Tsunami Hazards 20:57–94

Lane P, Donnelly JP, Woodruffe JD, Hawkes AD (2011) A decadally-resolved paleohurricane record archived in the late Holocene sediments of a Florida sinkhole. Mar Geol 287:14–30

Lanesky DE, Logan BW, Brown RG, Hine AC (1979) A new approach to portable vibracoring underwater and on land. J Sediment Petrol 49:654–657

Li X (1994) A 6200-year environmental history of the Pearl River Marsh, Louisiana. Dissertation, Louisiana State University

Li C, Weeks E, Rego J (2009) In situ measurements of saltwater flux through tidal passes of Lake Pontchartrain estuary by Hurricanes Gustav and Ike in September 2008. Geophys Res Lett 36:L19609

Liu K-B (2004) Paleotempestology: principles, methods, and examples from Gulf coast lake-sediments. In: Murnane R, Liu K (eds) Hurricanes and typhoons: past present and potential. Columbia Press, New York, pp 13–57

Liu K-B, Fearn ML (1993) Lake-sediment record of late Holocene hurricane activities from coastal Alabama. Geology 21:793–796

Liu K-B, Fearn ML (2000a) Holocene history of catastrophic hurricane landfalls along the Gulf of Mexico coast reconstructed from coastal lake and marsh sediments. In: Ning ZH, Abdollahi

KK (eds) Current stresses and potential vulnerabilities: Implications of Global Change for the Gulf Coast Region of the United States, Gulf Coast Regional Climate Change Council. Franklin Press, Baton Rouge, pp 38–47

Liu K-B, Fearn ML (2000b) Reconstruction of prehistoric landfall frequencies of catastrophic hurricanes in northwestern Florida from lake sediment records. Quatern Res 54:238–245

Liu K-B, Lu H, Shen C (2003) Assessing the vulnerability of the Alabama Gulf coast to intense hurricane strikes and forest fires in the light of long-term climatic changes. In: Ning ZH, Turner RE, Doyle T, Abdollahi K (eds) Integrated assessment of the consequences of climate change for the Gulf Coast region. Environmental Protection Agency, Baton Rouge, pp 223–230

Liu K-B, Li C, Bianchette TA, McCloskey TA, Yao Q, Weeks E (2011) Storm deposition in a coastal backbarrier lake in Louisiana caused by hurricanes Gustav and Ike. J Coast Res SI 64:1866–1870

Liu H, Zhang K, Li Y, Xie L (2013) Numerical study of the sensitivity of mangroves in reducing storm surge and flooding to hurricane characteristics in southern Florida. Cont Shelf Res 64:51–65

Malaizé B, Bertran P, Carbonel P, Bonnissent D, Charlier K, Galop D, Limbert D, Serrand N, Stouvenot C, Pujol C (2011) Hurricanes in the Caribbean during the past 3700 years BP. Holocene 21:911–924

Mann ME, Emanuel K (2006) Atlantic hurricane trends linked to climate change. Eos Trans Am Geophys Union 87:233–241

Mann ME, Woodruff JD, Donnelly JP, Zhang Z (2009) Atlantic hurricanes and climate over the past 1,500 years. Nature 460:880–885

McCloskey TA, Keller G (2009) 5000 year sedimentary record of hurricane strikes on the central coast of Belize. Quatern Int 195:53–68

McCloskey TA, Liu K-B (2012) A 7000 year record of paleohurricane activity from a coastal wetland in Belize. Holocene 23:278–291

McIvor AL, Möller I, Spencer T, Spalding M (2012) Reduction and wind and swell waves by mangroves. NCP Report 1. Cambridge Coastal Research Unit Working Paper 40: 1–27

Montaggioni L, Braithwaite CJR (2009) Quaternary Coral Reef Systems. Developments in Marine Geology 5. Elsevier, Amsterdam

Morton RA (2002) Factors controlling storm impacts on coastal barriers and beaches—a preliminary basis for near real-time forecasting. J Coast Res 18:486–501

Morton RA, Gelfenbaum G, Jaffe BJ (2007) Physical criteria for distinguishing sandy tsunami and storm deposits using modern examples. Sediment Geol 200:184–207

Morton RA, Richmond BM, Jaffe BE, Gelfenbaum G (2008) Coarse-clast ridge complexes of the Caribbean: a preliminary basis for distinguishing tsunami and storm-wave origins. J Sediment Res 78:624–637

Murnane RJ (2004) Introduction. In: Murnane R, Liu K (eds) Hurricanes and typhoons: past present and potential. Columbia Press, New York, pp 1–10

National Oceanic and Atmospheric Administration (NOAA) (2015) National Hurricane Center. NHC Data Archive. Past Track Seasonal Maps. Atlantic Basin (http://www.nhc.noaa.gov/data/#tracks_all)

Nichols MM, Boon JD (1994) Sediment transport processes in coastal lagoons. In: Kjerfve B (ed) Coastal lagoon processes. Elsevier, Amsterdam, pp 157–219

O'Loughlin KF, Lander JF (2003) Caribbean tsunamis. A 500 year history from 1498–1998. Advances in Natural and Technological Hazards Research. Kluwer Academic Publishers, Dordrecht

Otvos EG (1999) Quaternary costal history, basin geometry and assumed evidence for hurricane activity, northeastern Gulf of Mexico coastal plain. J Coast Res 15:438–443

Otvos EG (2001) Assumed Holocene highstands, Gulf of Mexico. Basic issues of sedimentary and landform criteria. J Sediment Res 71:645–647

Otvos EG (2002) Discussion of "Prehistoric landfall frequences of catastrophic hurricanes" (Liu and Fearn, 2000). Quatern Res 57:425–428

Parker RH (1959) Macro-invertebrate assemblages of central Texas coastal bays and Laguna Madre. AAPG Bull 43:2100–2166

Peters R, Jaffe BE (2010) Identification of tsunami deposits in the geologic record; developing criteria using recent tsunami deposits. U.S. Geological Survey Open-File Report 2010-1239

Pilarczyk JE, Reinhardt EG (2011) *Homotrema rubrum* (Lamarck) taphonomy as an overwash indicator in marine ponds from Anegada, British Virgin Islands. Nat Hazards 63:85–100

Purdy EG, Gischler E (2003) The Belize margin revisited: 1. Holocene marine facies. Int J Earth Sci 92:532–551

Purdy EG, Pusey WC, Wantland KF (1975) Continental shelf of Belize: regional shelf attributes. In: Wantland KF, Pusey WC (eds) Belize shelf-carbonate sediments, clastic sediments, and ecology, AAPG Stud Geol 2, pp 1–40

Pusey WC (1975) Holocene carbonate sedimentation on northern Belize shelf. In: Wantland KF, Pusey WC (eds) Belize shelf-carbonate sediments, clastic sediments, and ecology, AAPG Stud Geol 2, pp 131–233

Santer BD, Wigley TML, Gleckler PJ, Bonfils C, Wehner MF, AchutaRao K, Barnett TP, Boyle JS, Brüggemann W, Fiorino M, Gillett N, Hansen JE, Jones PD, Klein SA, Meehl GA, Raper SCB, Reynolds RW, Taylor KE, Washington WM (2006) Forced and unforced ocean temperature changes in Atlantic and Pacific tropical cyclogenesis regions. Proc Natl Acad Sci 103:13905–13910

Saunders MA, Lea AS (2008) Large contribution of sea surface warming to recent increase in Atlantic hurricane activity. Nature 451:557–560

Scheffers A (2006) Sedimentary impacts of Holocene tsunami events from the intra Americas seas and southern Europe: a review. Z Geomorphol 146:7–37

Scheffers A, Kelletat D (2003) Sedimentologic and geomorphologic tsunami imprints worldwide—a review. Earth Sci Rev 63:83–92

Schwartz RK (1975) Nature and genesis of some washover deposits. U.S. Army Coastal Engineering Research Center Technical Memo 61, Ft. Belvoir, VA

Scott MR (1975) Distribution of clay minerals on Belize shelf. In: Wantland KF, Pusey WC (eds) Belize shelf-carbonate sediments, clastic sediments, and ecology. AAPG Stud Geol 2, pp 97–130

Scott DB, Collins ES, Gayes PT, Wright E (2003) Records of prehistoric hurricanes on the south Carolina coast based on micropaleontological and sedimentological evidence, with comparison to other Atlantic coast records. Geol Soc Am Bull 115:1027–1039

Sedgwick PE, Davis RA (2003) Stratigraphy of washover deposits in Florida: implications for recognition in the stratigraphic record. Mar Geol 200:31–48

Spiske M, Jaffe BE (2009) Sedimentology and hydrodynamic implications of a coarse-grained hurricane sequence in a carbonate reef setting. Geology 37:839–842

Spiske M, Böröcz Z, Bahlburg H (2008) The role of porosity in discriminating tsunami and hurricane emplacement of boulders—a case study from the Lesser Antilles, southern Caribbean. Earth Planet Sci Lett 268:384–396

Stoddart DR (1962) Catastrophic storm effects on the British Honduras reefs and cays. Nature 196:512–515

Switzer AD, Jones BG (2008) Large-scale washover sedimentation in a freshwater lagoon from the southeast Australian coast: sea-level change, tsunami or exceptionally large storm? Holocene 18:787–803

Talma AS, Vogel JC (1993) A simplified approach to calibrating ^{14}C dates. Radiocarbon 35:317–322

Turney WJ, Perkins BF (1972) Molluscan distribution in Florida Bay. Sedimenta III. University of Miami, Miami

Tuttle MP, Ruffman A, Anderson T, Jeter H (2004) Distinguishing tsunami from storm deposits in eastern North America: the 1929 Grand Banks Tsunami versus the 1991 Halloween Storm. Seismol Res Lett 75:117–131

Wallace DJ, Woodruff JD, Anderson JB, Donnelly JP (2014) Palaeohurricane reconstructions from sedimentary archives along the Gulf of Mexico, Caribbean Sea and western North Atlantic Ocean margins. In: Martini IP, Wanless HR (eds) Sedimentary coastal zones from high to low latitudes: similarities and differences, Geol Soc SP 388, London, pp 481–502

Webster PJ, Holland GJ, Curry JA, Chang HR (2005) Changes in tropical cyclone number, duration, and intensity in a warming environment. Science 309:1844–1846

Williams HFL (2010) Storm surge deposition by Hurricane Ike on the McFaddin National Wildlife Refuge, Texas: implications for paleotempestology studies. J Foramin Res 40:210–219

Woodruff JD, Donnelly D, Emanuel K, Lane P (2008a) Assessing sedimentary records of paleo-hurricane activity using modeled hurricane climatology. Geochem Geophys Geosyst 9:Q09V10

Woodruff JD, Donnelly D, Mohrig D, Geyer WR (2008b) Reconstructing relative flooding intensities responsible for hurricane-induced deposits from Laguna Playa Grande, Vieques, Puerto Rico. Geology 36:391–394

Wooller MJ, Behling H, Guerrero JL, Jantz N, Zweigert ME (2009) Late Holocene hydrologic and vegetation changes at Turneffe atoll, Belize, compared with records from mainland central America and Mexico. Palaios 24:650–656

Wright ACS, Romney DH, Arbuckle RH, Vial DE (1959) Land in British Honduras. Colonial Research Publications 24, London

Zhang R, Delworth TL (2006) Impact of Atlantic multidecadal oscillations on India/Sahel rainfall and Atlantic hurricanes. Geophys Res Lett 33:L17712

Zhang R, Delworth TL (2009) A new method for attributing climate variations over the Atlantic Hurricane basin's main development region. Geophys Res Lett 36:L06701

Zhang K, Liu H, Li Y, Xu H, Shen J, Rhome J, Smith TJ III (2012) The role of mangroves in attenuation of storm surges. Estuar Coast Shelf Sci 102–103:11–23

Zhou X (1998) A 4,000-year pollen record of vegetation changes, sea-level rise, and hurricane disturbance in Atchafalaya Marsh of Southern Louisiana. Dissertation, Louisiana State University